High-speed optical GEM readout

F. M. Brunbauer
on behalf of the CERN EP-DT-DD GDD team

RD51 collaboration meeting
June 20, 2018

Optical readout

Intuitive pixelated readout with
megapixel imaging sensors

High spatial **resolution**

Integrated imaging approach

Lenses and mirrors to enable
adjustable magnification and camera location

Frame rate

Radiation hardness of imaging sensors

Need of **CF_4**-based gas mixtures
or wavelength shifters

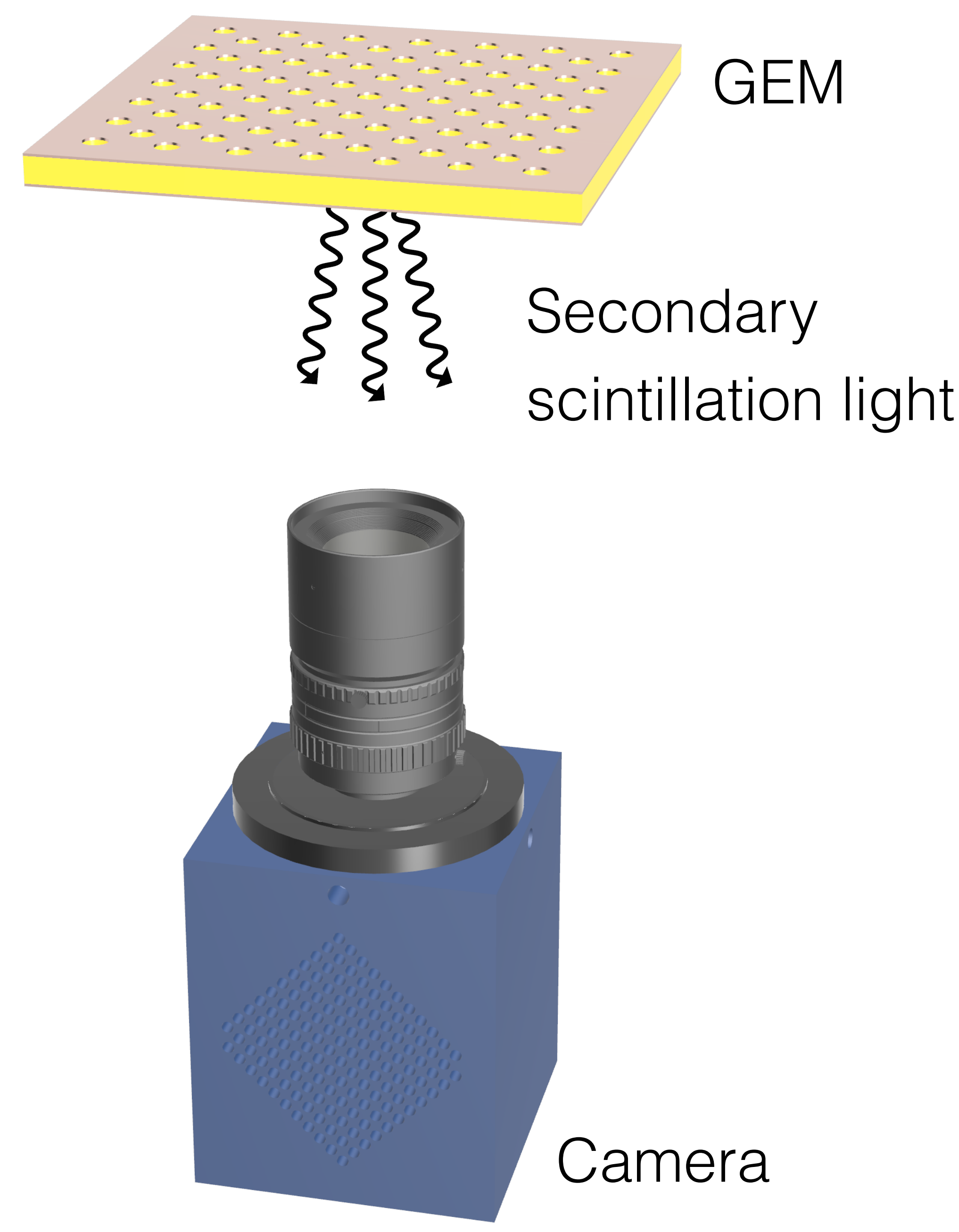

Optical readout

Intuitive pixelated readout with
megapixel imaging sensors

High spatial **resolution**

Integrated imaging approach

Lenses and mirrors to enable
adjustable magnification and camera location

Frame rate

Radiation hardness of imaging sensors

Need of **CF_4**-based gas mixtures
or wavelength shifters

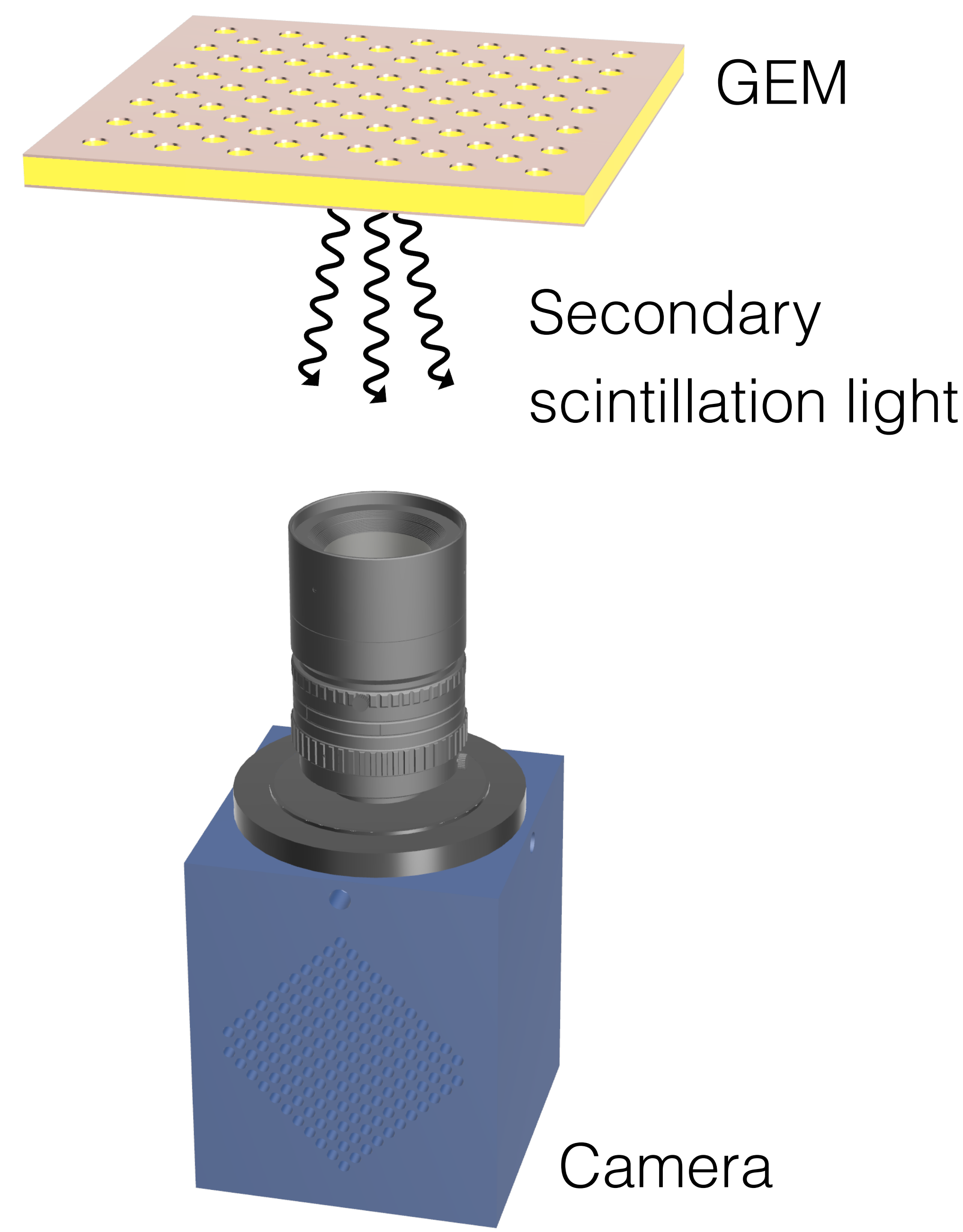

Frame rate

CCD
7 Hz frame rate

sCMOS
100 Hz frame rate

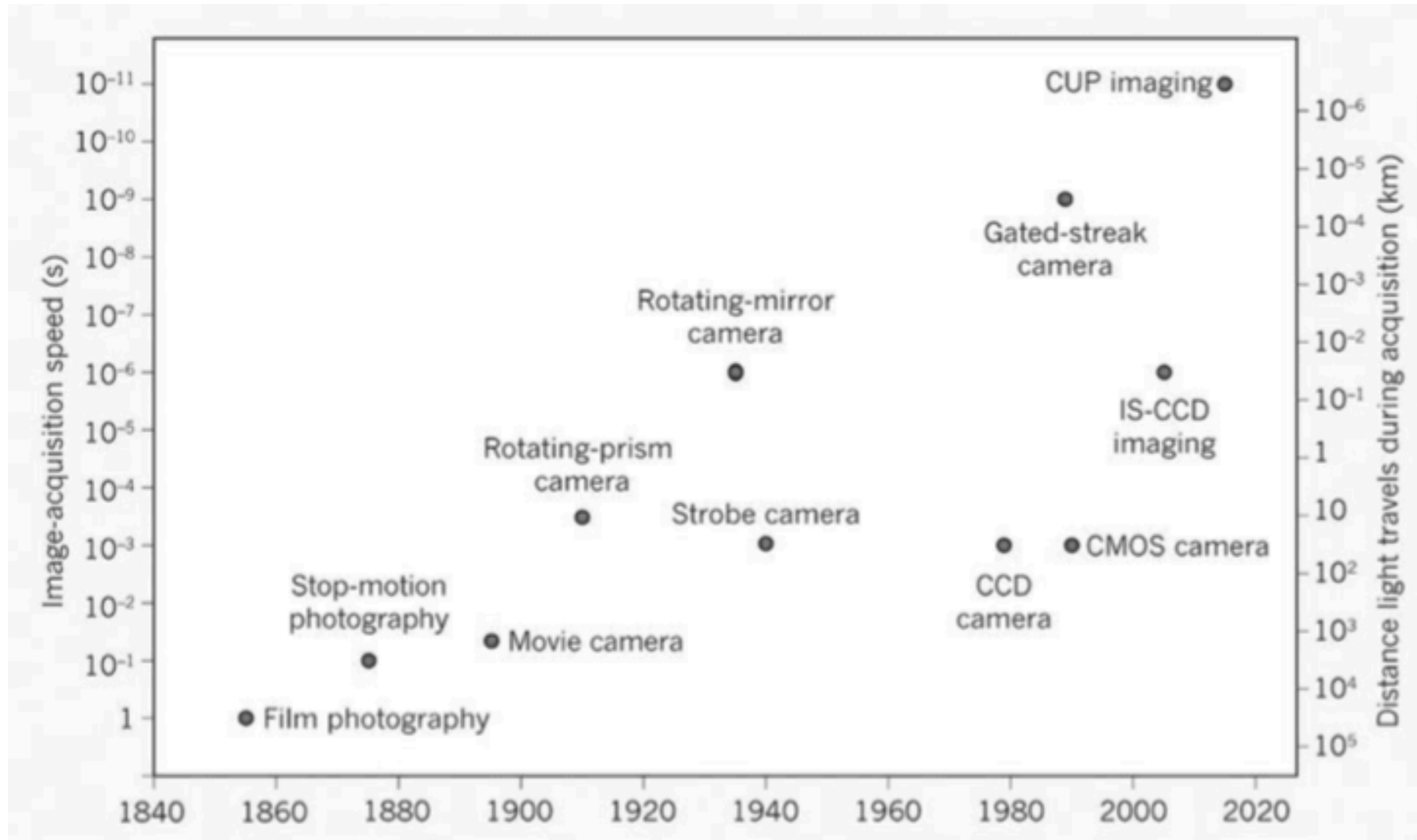

Image adapted from: B. Pogue, Nature 516 (2014) 46–47

Frame rate

CCD
7 Hz frame rate

sCMOS
100 Hz frame rate

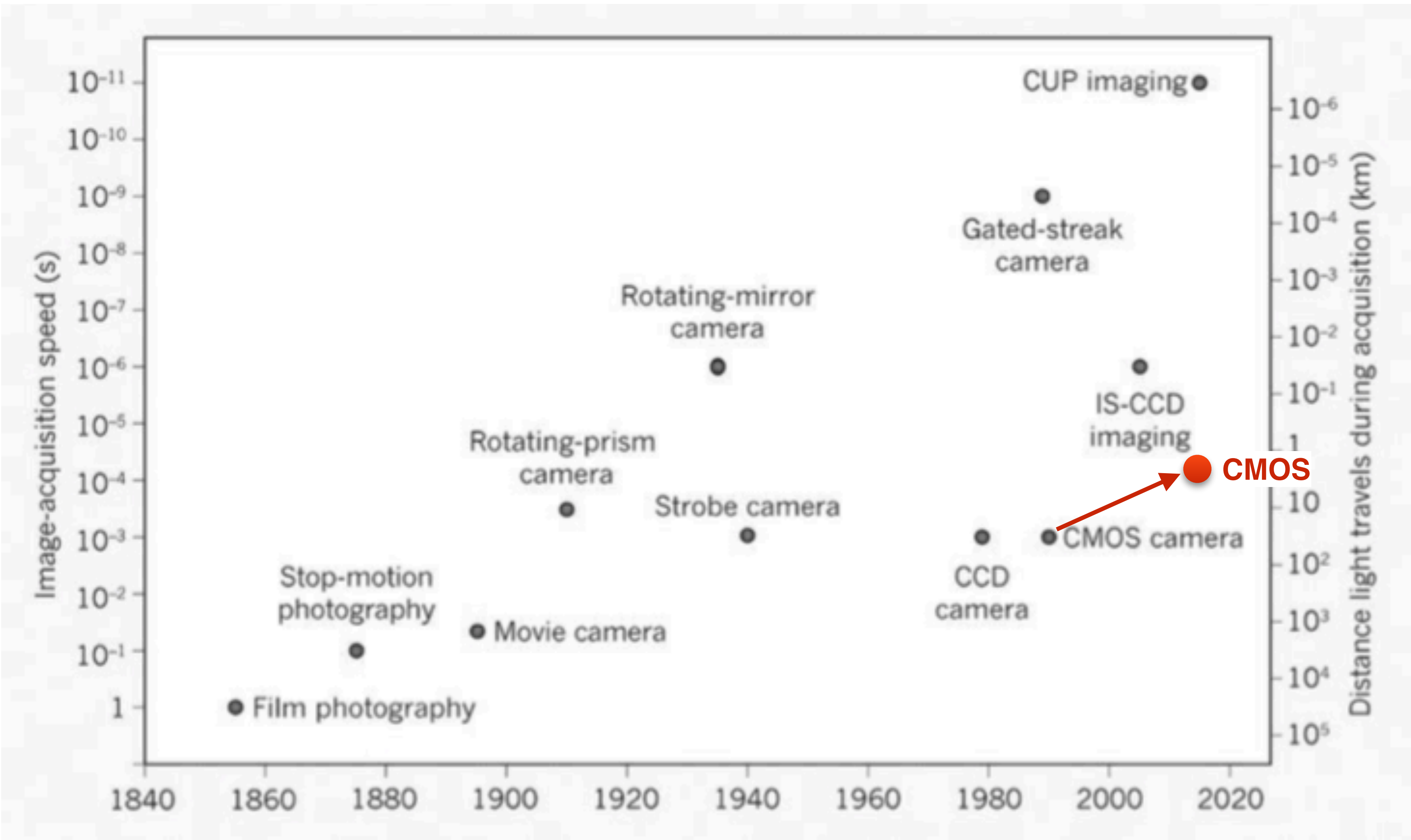

Image adapted from: B. Pogue, Nature 516 (2014) 46–47

High-speed CMOS cameras

Photron FASTCAM SA-Z

H \ V	56	48	40	32	24	16	8
1024	300.000	336.000	360.000	450.000	525.000	672.000	900.000
896	315.000	360.000	400.000	480.000	560.000	720.000	900.000
768	360.000	400.000	450.000	525.000	630.000	800.000	1.008.000
640	400.000	450.000	525.000	600.000	720.000	840.000	1.008.000
512	480.000	525.000	600.000	700.000	800.000	900.000	1.200.000
384	525.000	630.000	720.000	800.000	900.000	1.008.000	1.400.000
256	700.000	720.000	840.000	900.000	1.008.000	1.200.000	1.400.000
128	900.000	900.000	1.008.000	1.200.000	1.200.000	1.440.000	2.100.000

- 1 megapixel CMOS sensor
- 12 bit depth
- **20 kfps** at full resolution
- **2.1 Mfps** at 128x8
- ISO 50,000 sensitivity

Phantom v2512

Resolution	FPS
1280 x 800	25,700
1280 x 720	28,500
1024 x 512	47,400
640 x 480	70,100
512 x 384	99,800
256 x 256	206,300
256 x 128	380,100
128 x 64	783,100
128 x 32	1,000,000
128 x 16	1,000,000

- 1 megapixel CMOS sensor
- 12 bit depth
- **25 kfps** at full resolution
- **1 Mfps** at 128x32
- ISO 100,000 sensitivity

High-speed CMOS cameras

Ar/CF_4 gas mixtures feature ample visible scintillation light emission with a peak around **630 nm**

The response of high-speed CMOS is compatible with the scintillation light emission from **Ar/CF_4**

The Phantom v2512 CMOS sensor features a peak quantum efficiency of about 50% at 650 nm

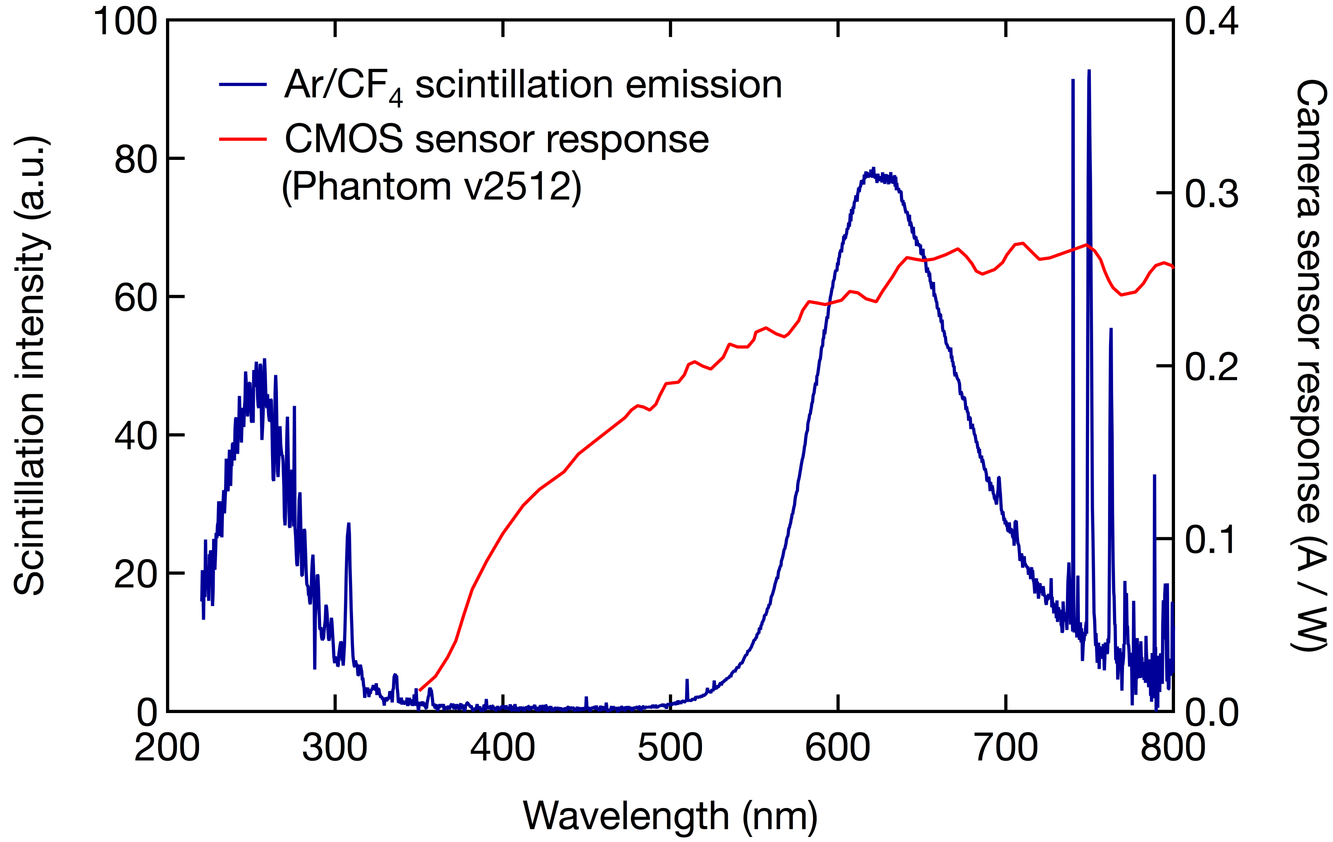

X-ray fluoroscopy

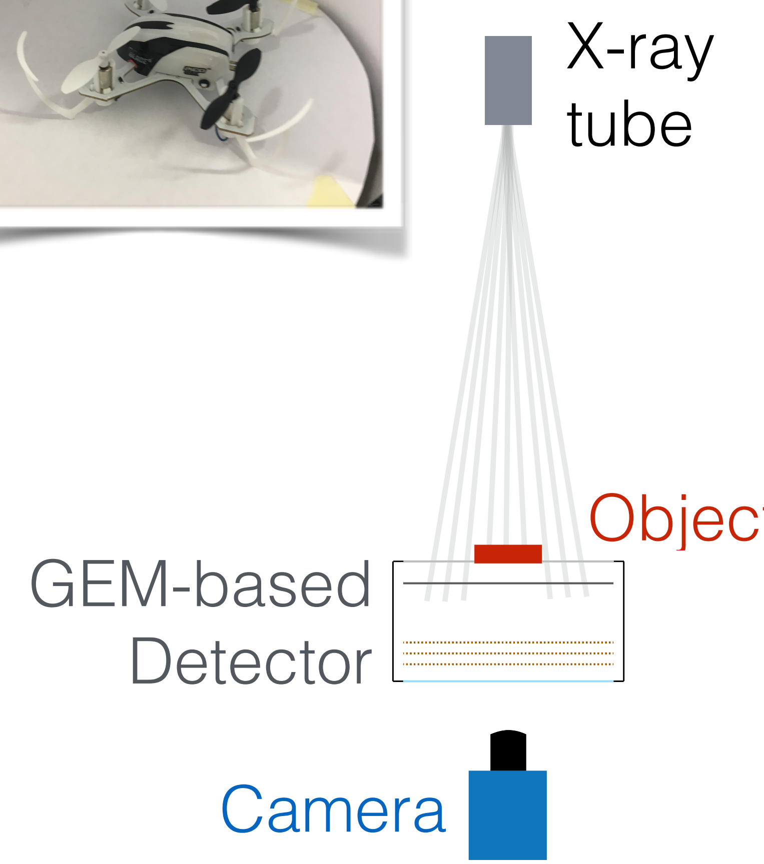

2 kfps, 40kV - 40mA X-rays, quad-GEM at 400V

Minimising motion blur and enabling fast radiography due to fast sensor readout and sensitivity

X-ray fluoroscopy

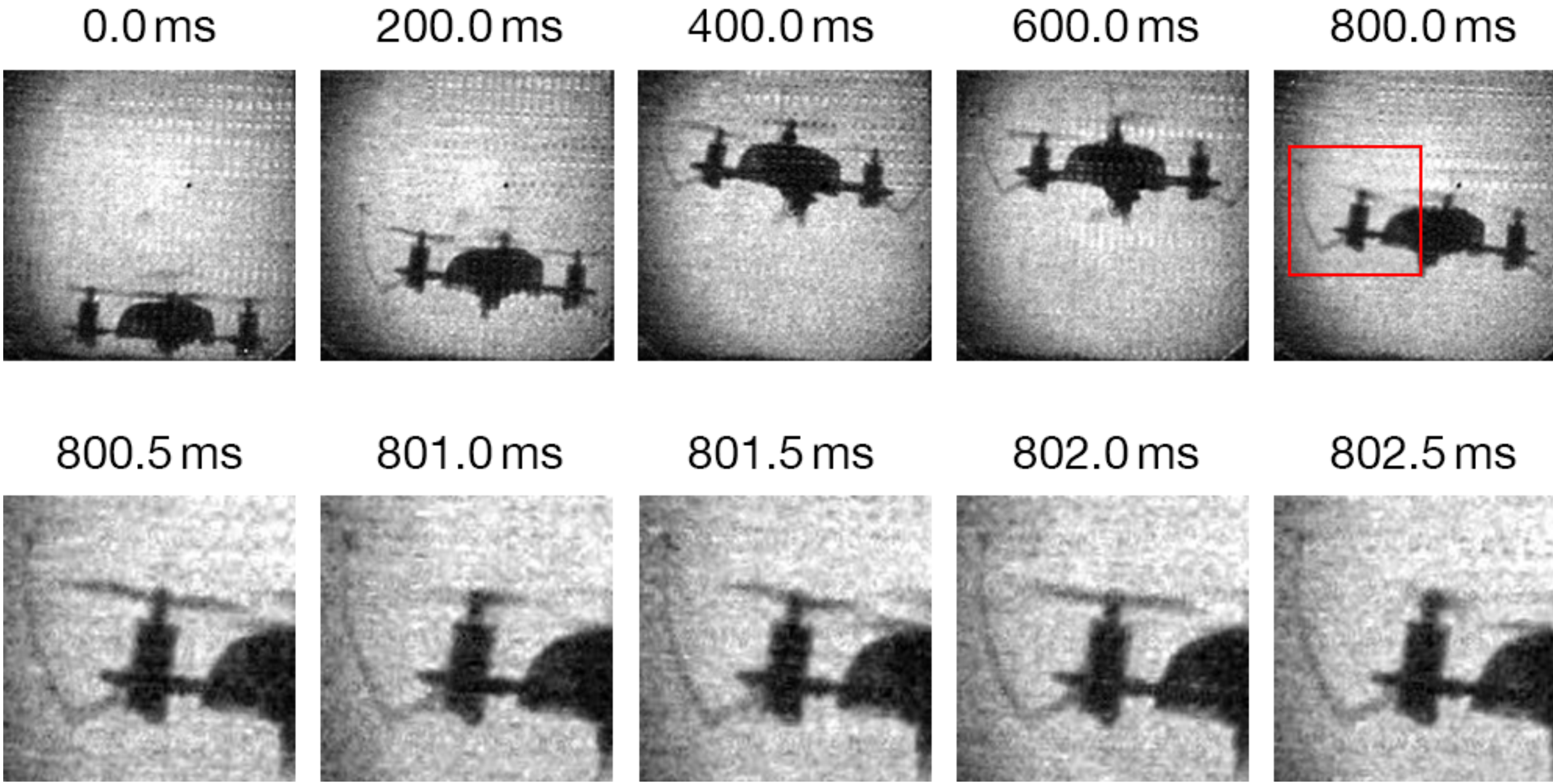

2 kfps, 40kV - 40mA X-rays, quad-GEM at 400V
Minimising motion blur and enabling fast radiography due to sensor readout and sensitivity

Beam monitoring

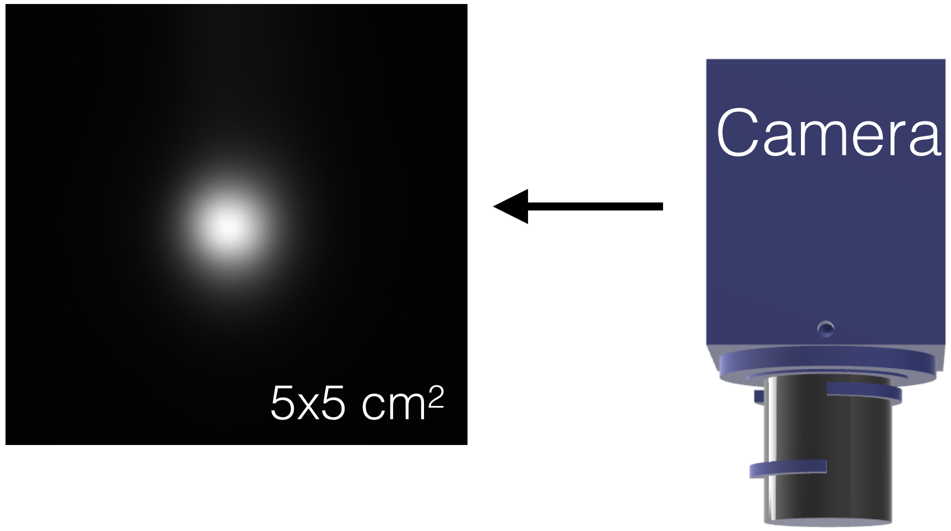

Tens of kHz at 1 Mpx readout
Fast readout enables direct feedback on beam position and profile

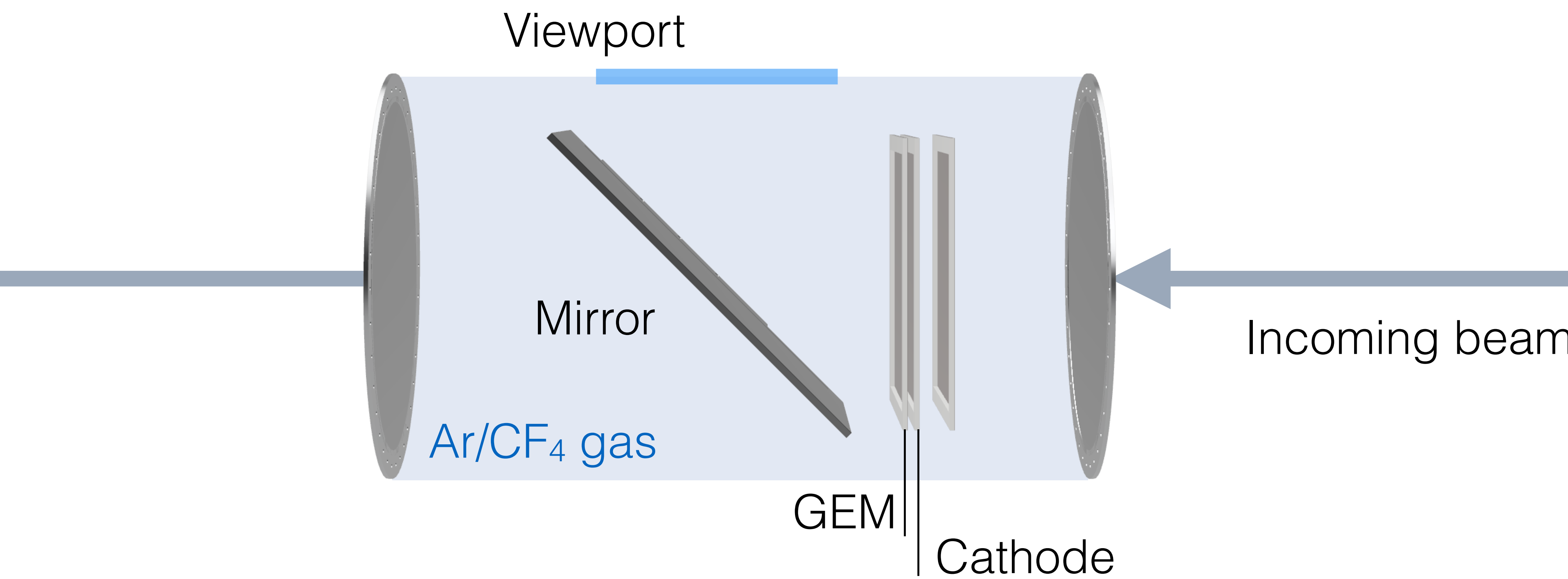

Next step:
Evaluate possibility of on-camera imaging processing for sparse readout and active feedback

Optically read out TPC

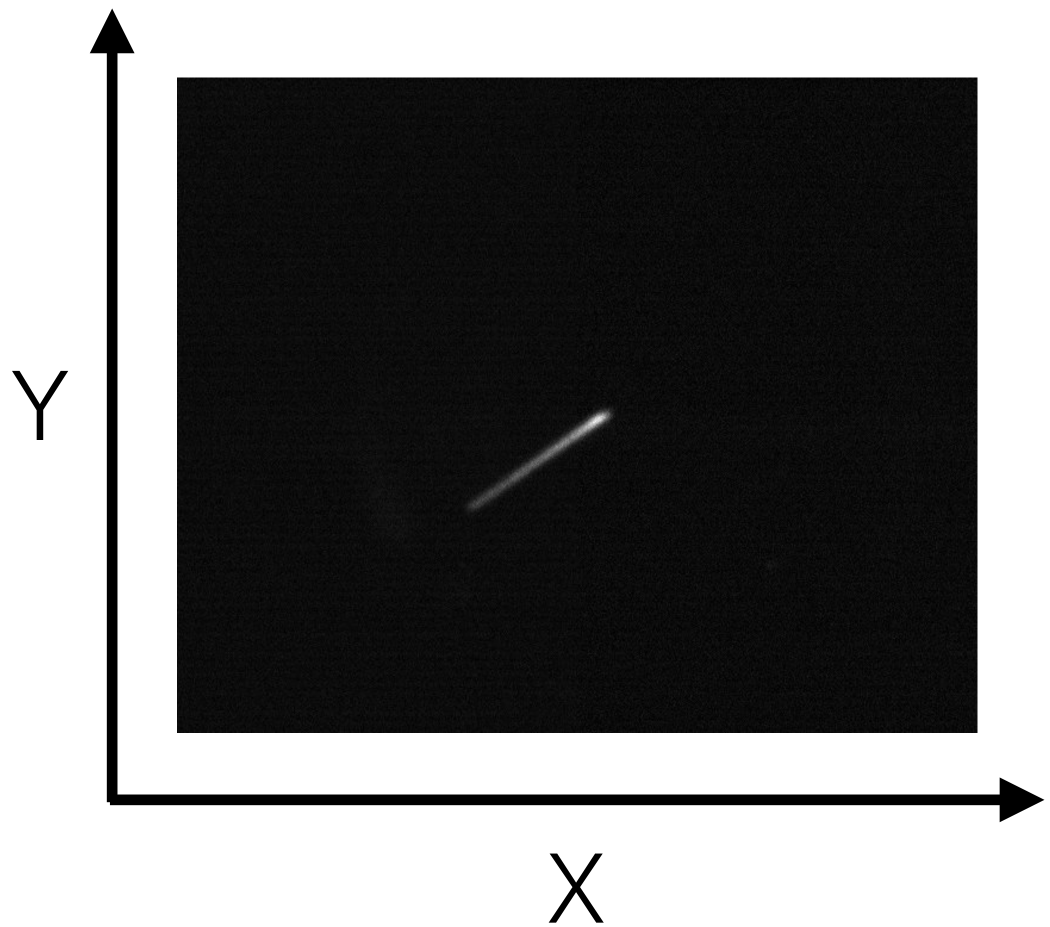

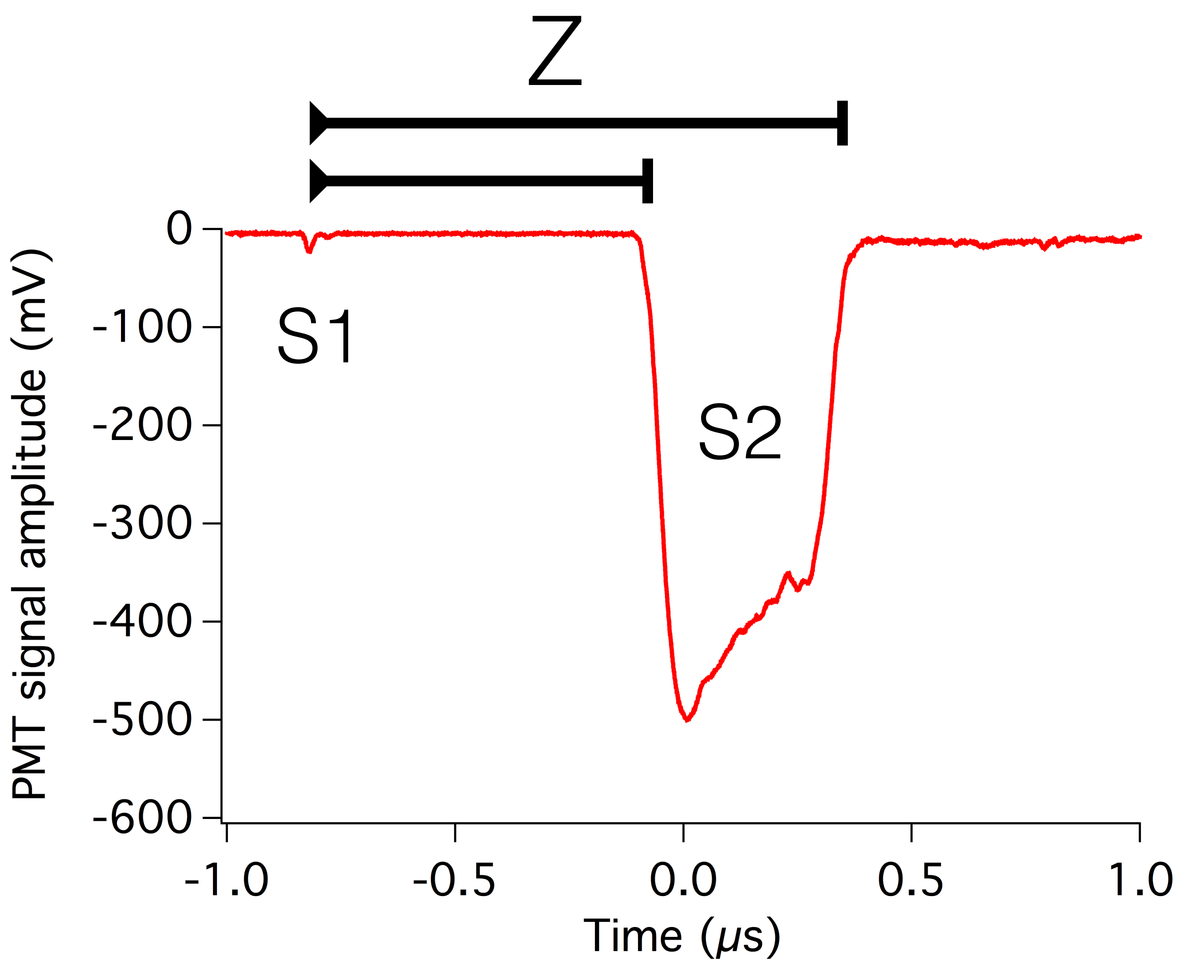

PMT waveform

Depth information can be determined from time between primary (S1) and secondary (S2) scintillation and width of S2 signal

Optically read out TPC

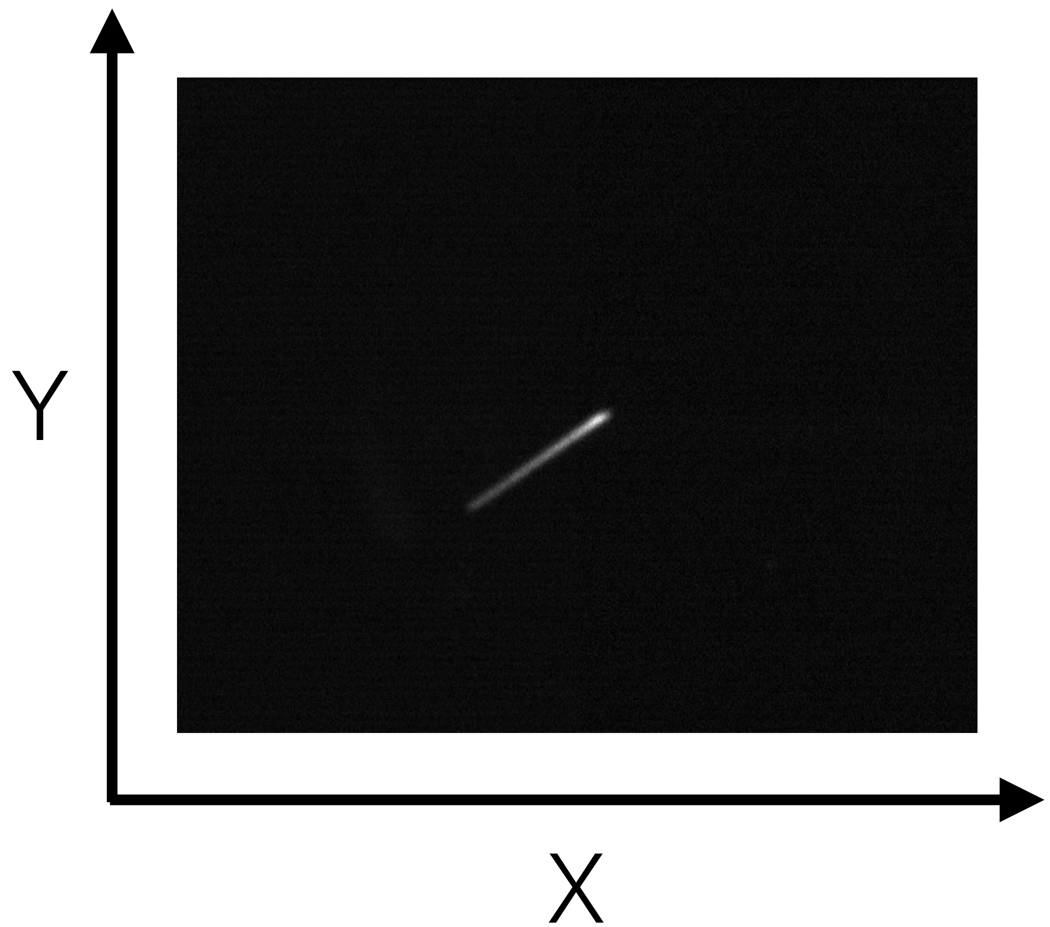

Electron drift velocity in Ar/CF_4 80/20%

Christophorou et al., 1979

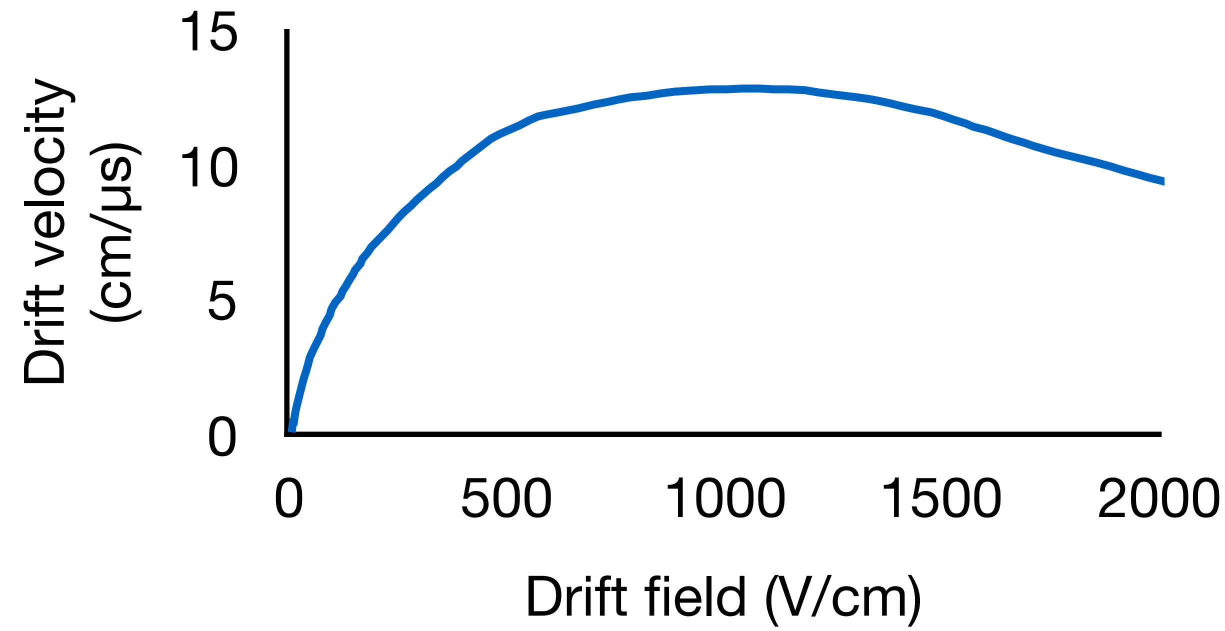

At **very low drift fields**, the arrival time of primary electrons at the GEM in a TPC setup can be resolved in **individual image frames**

From the known time difference between frames, the depth of interaction at a certain 2D location can be determined

3D alpha track reconstruction

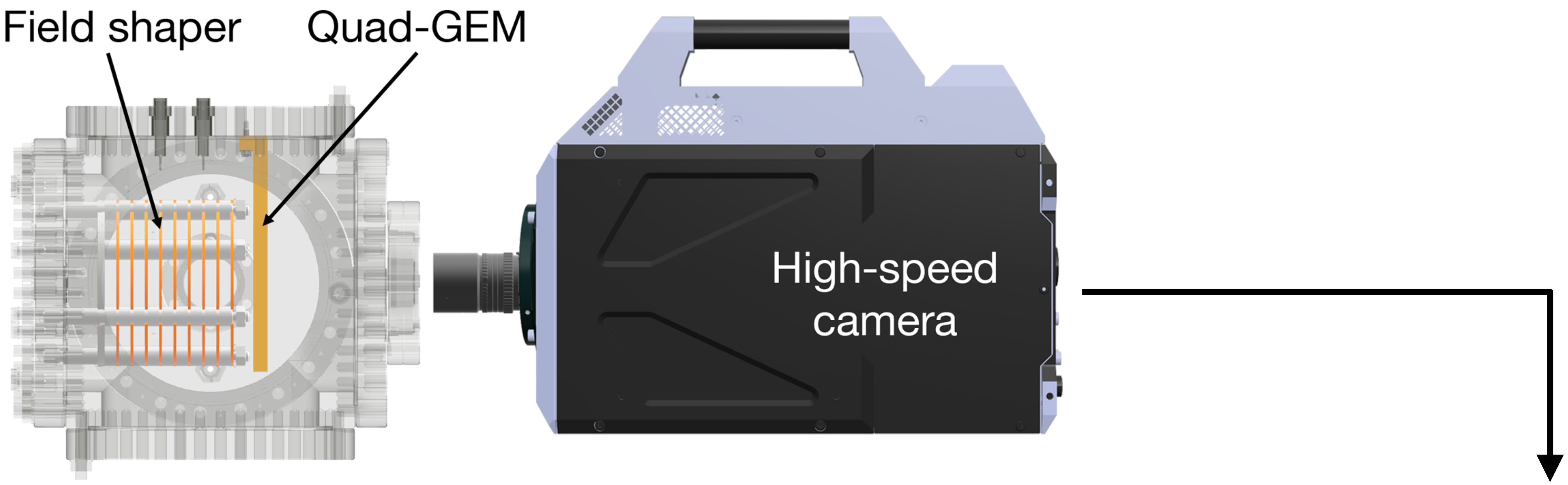

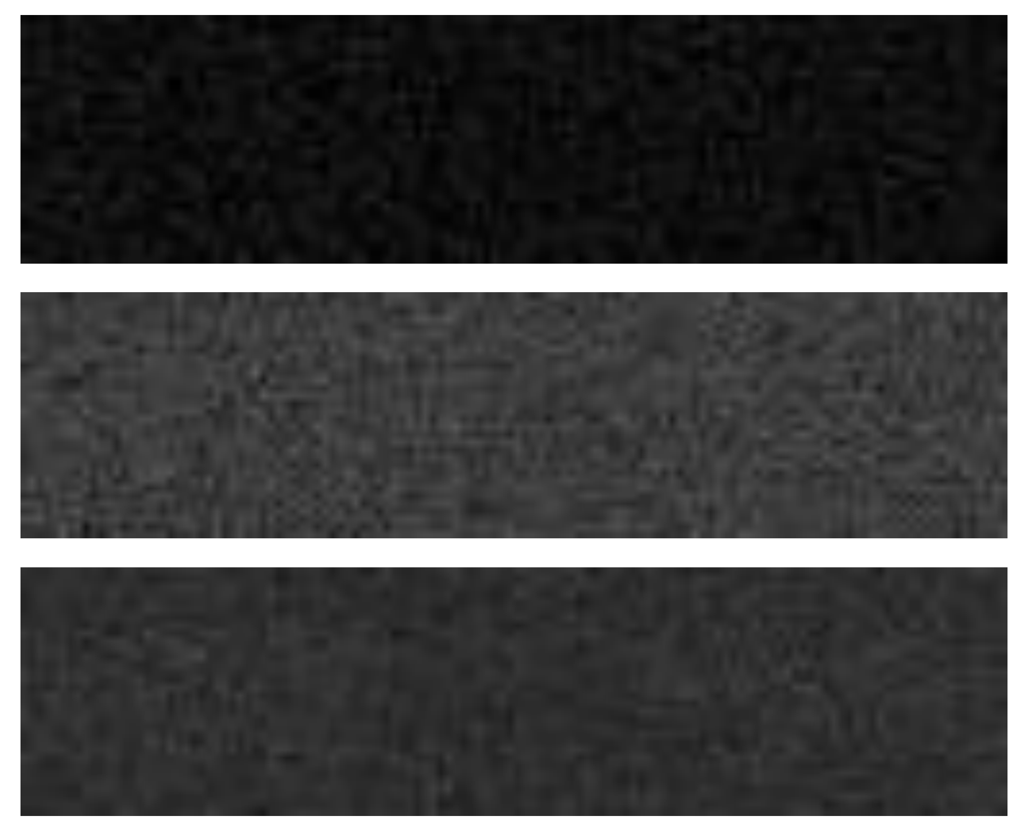

At very low drift fields, the arrival time of primary electrons at the GEM in a TPC setup can be resolved in individual image frames

From the known time difference between frames, the depth of interaction at a certain 2D location can be determined

3D alpha track reconstruction

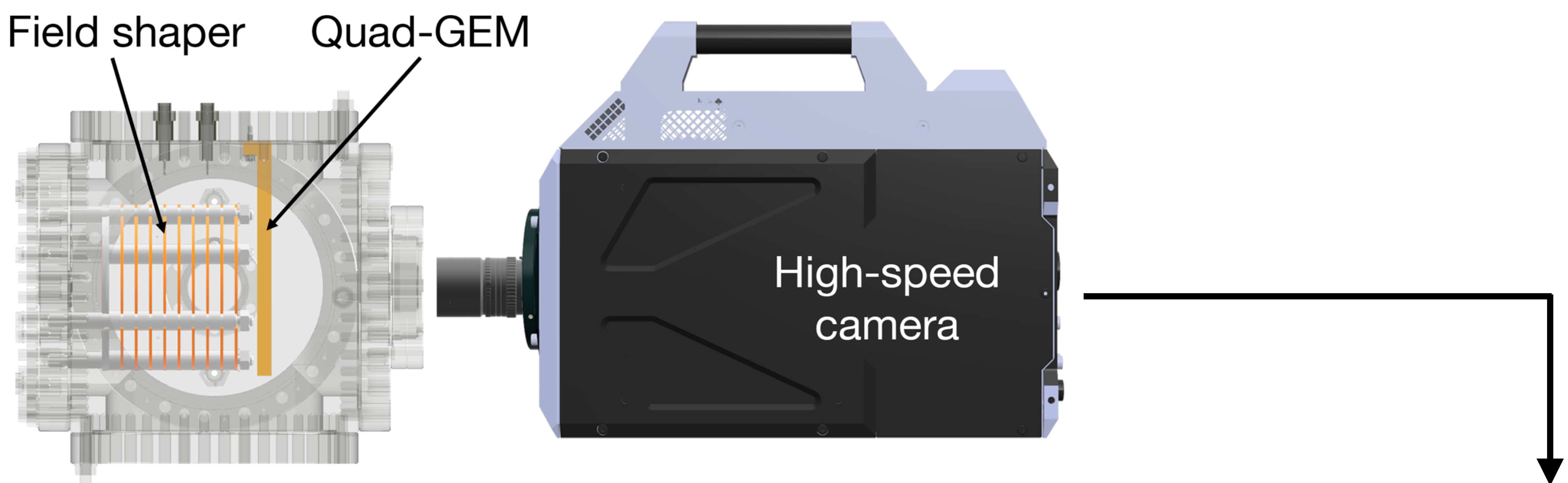

At very low drift fields, the arrival time of primary electrons at the GEM in a TPC setup can be resolved in individual image frames

From the known time difference between frames, the depth of interaction at a certain 2D location can be determined

3D alpha track reconstruction

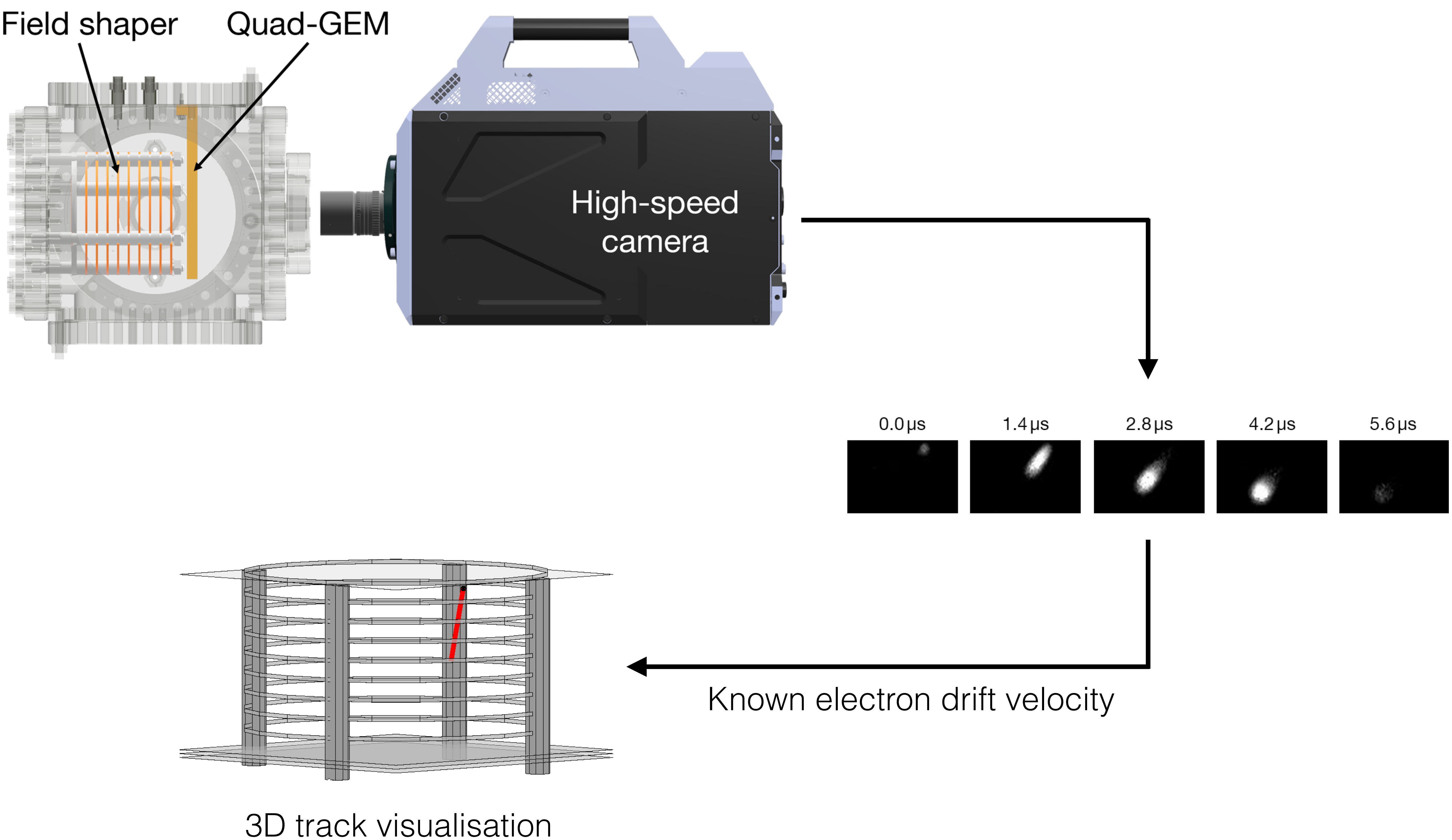

X-ray photon sensitivity

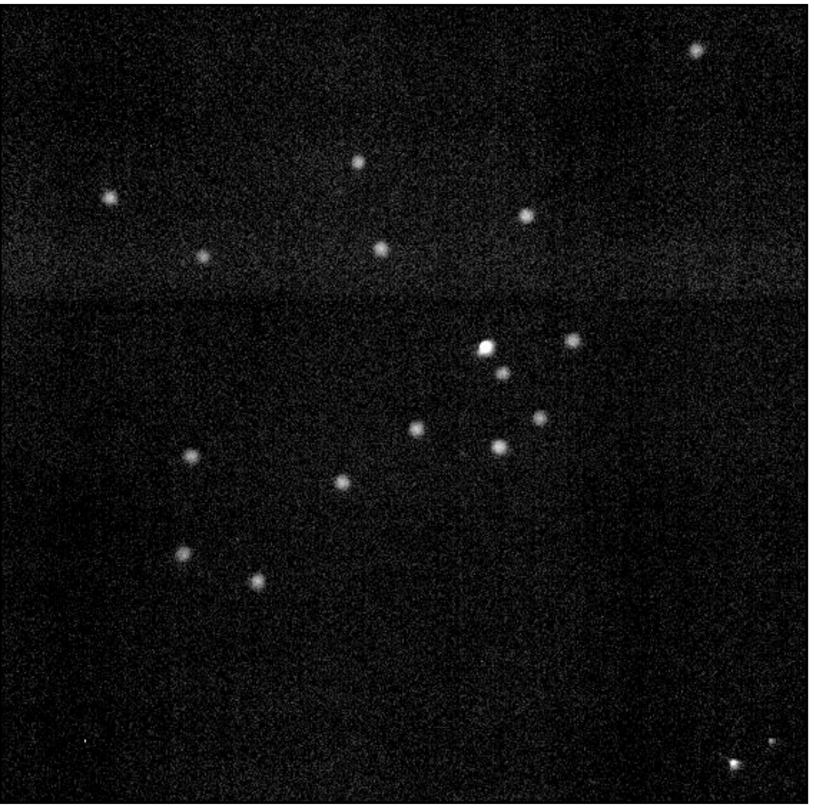

Individual frame

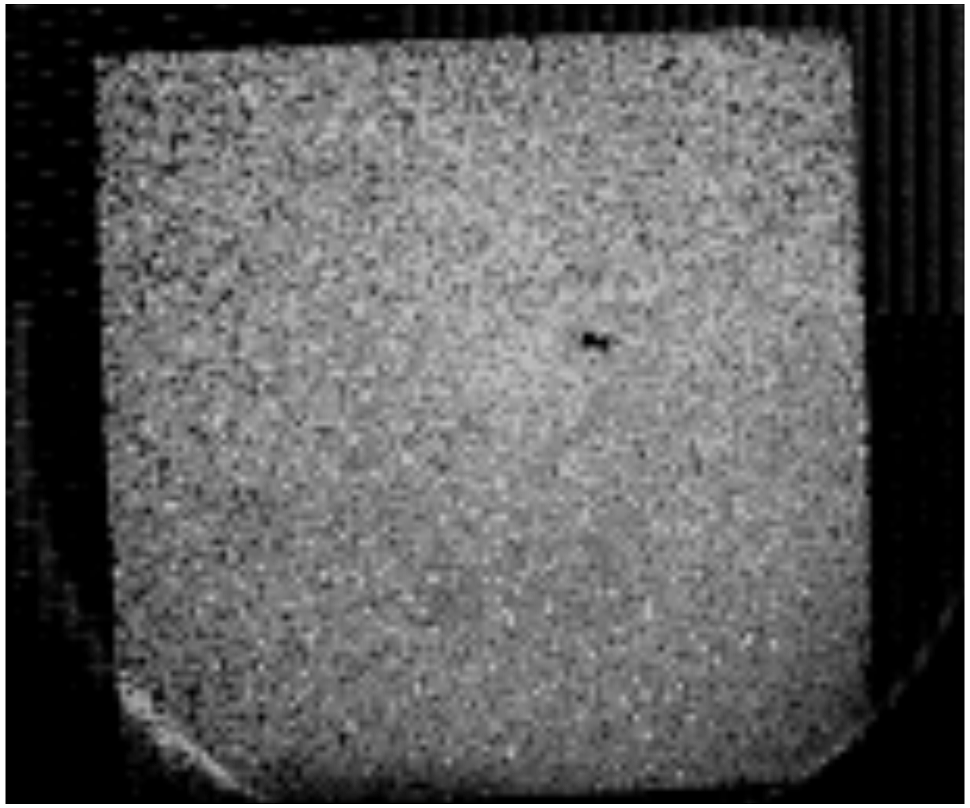

Integrated exposure

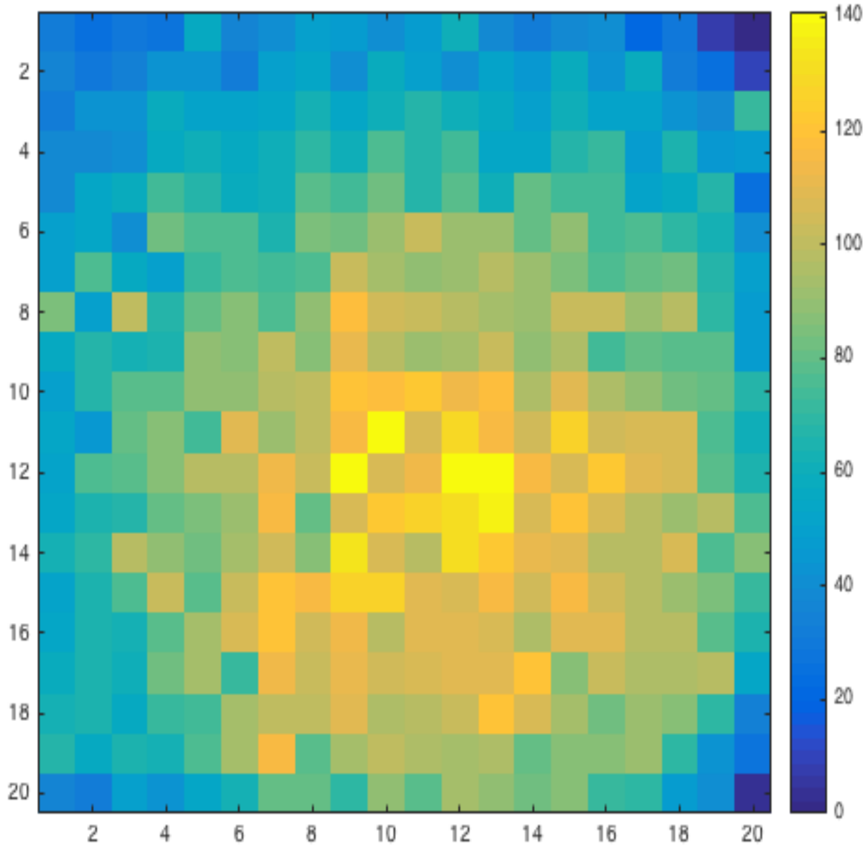

Calculated hitmap

Potential application:
Full-field X-ray fluoroscopy with energy sensitivity and large active area

10 kfps, 55Fe, GEMs at 400V, 4x4 software binning

X-ray photon sensitivity

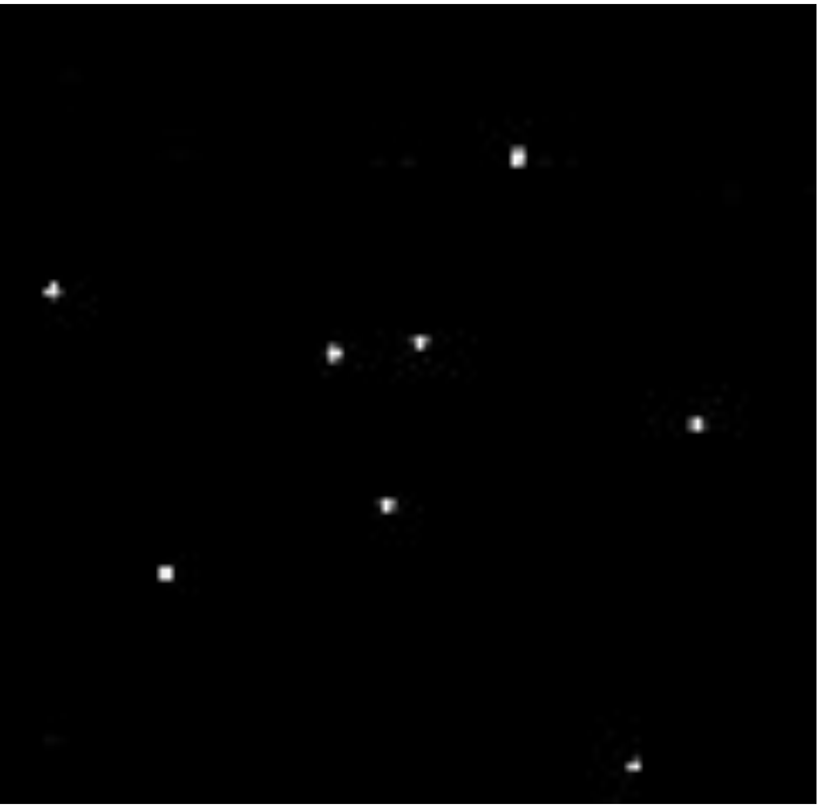

Individual frame

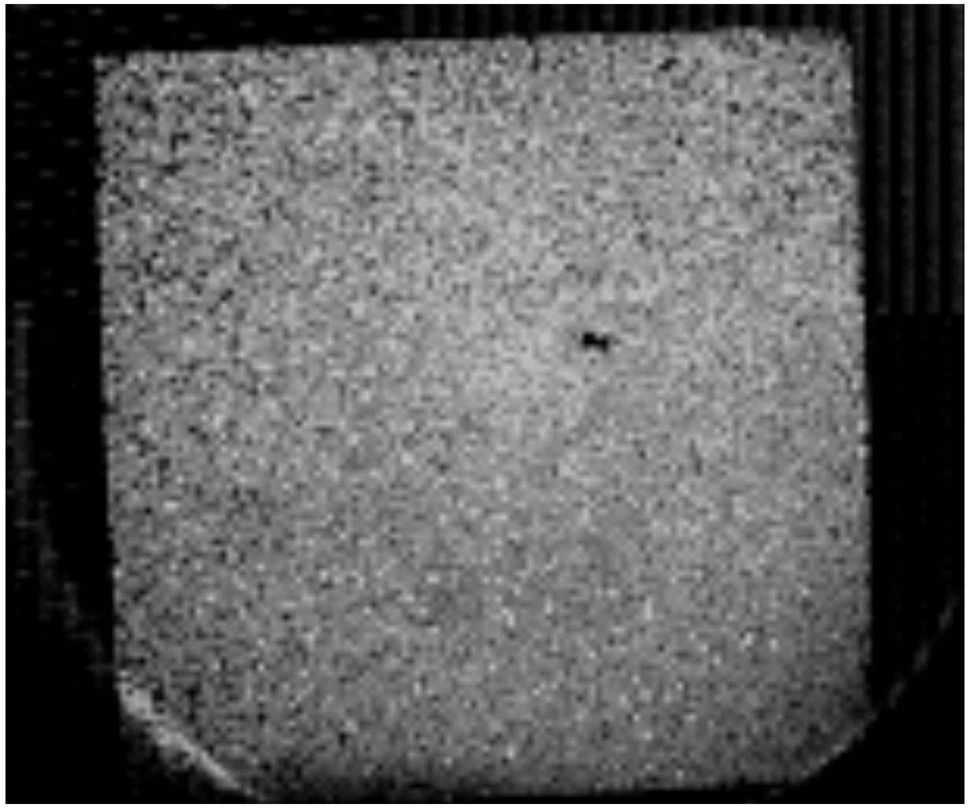

Integrated exposure

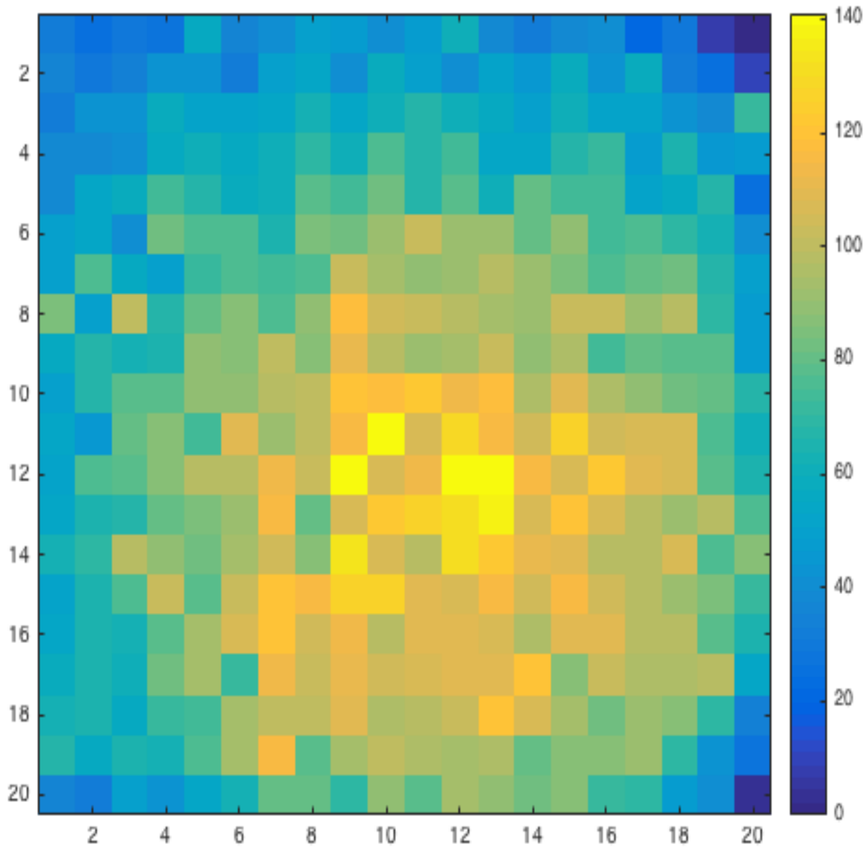

Calculated hitmap

Potential application:
Full-field X-ray fluoroscopy with energy sensitivity and large active area

10 kfps, 55Fe, GEMs at 400V, 4x4 software binning

Conclusions

Ultra-fast CMOS cameras enable novel readout approaches and offer high sensitivity

Imaging at **1 Mfps** enables imaging at time scales compatible with drift times and enables **3D reconstruction** in a TPC

On-camera **image processing** might enable active feedback beam monitoring systems

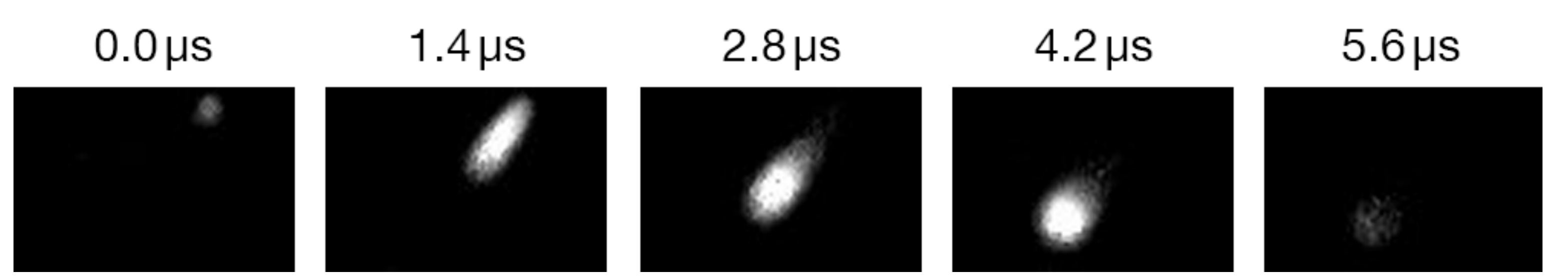

3D printing of functional detector components

F. M. Brunbauer
on behalf of the CERN EP-DT-DD GDD team

RD51 collaboration meeting
June 20, 2018

Additive manufacturing

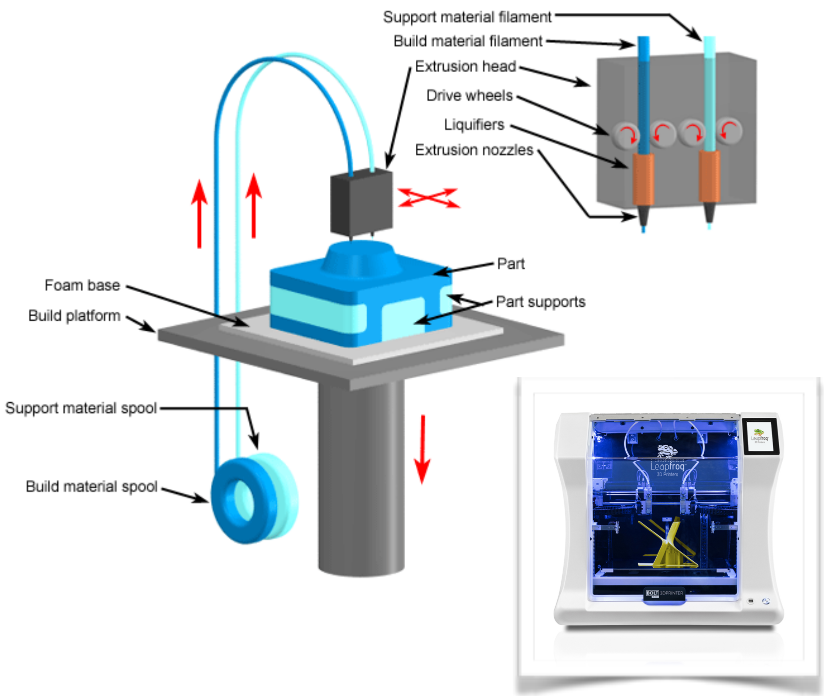

Image from: http://www.custompartnet.com/wu/fused-deposition-modeling and from www.lpfrg.com

Fused filament fabrication

Leapfrog Bolt

Specifications:
400 μm traces
Max. object size: 30x30x20cm^2

Conductivity: 100 - 0.6 Ω cm

Accessible: ≈5 k€

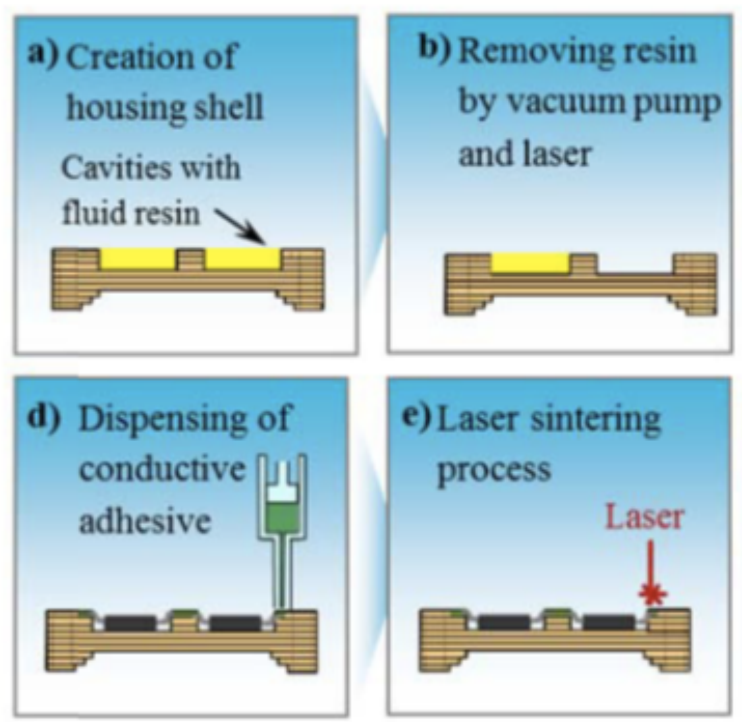

Image adapted from B. Niese et al. Physics Procedia 56 (2014) 336 – 344

Stereolithograhy + Selective laser sintering

B. Niese et al. Physics Procedia **56** (2014) 336 – 344

Silver-filled, solvent-free conductive adhesive
High conductivity
Experimental hybrid technique

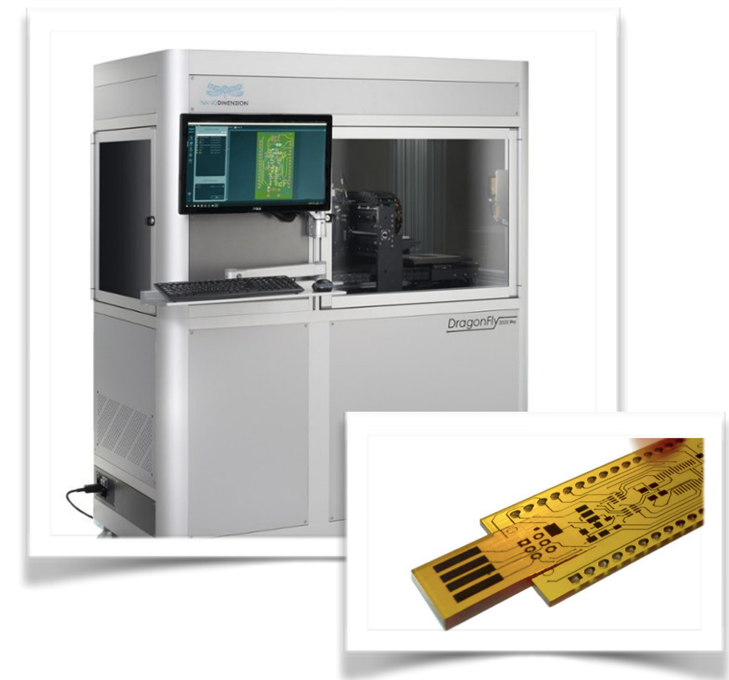

Images from nano-di.com

Functional Nano Inks

DragonFly™ 2020 Pro 3D Printer

Specifications:
100 μm traces
Min. object size: 400 μm
Min. Layer thickness: 12 μm
Expensive: ≈250 k€

Potential geometries

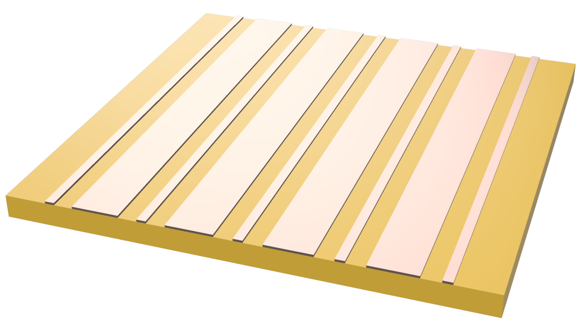

MSGC-like structure

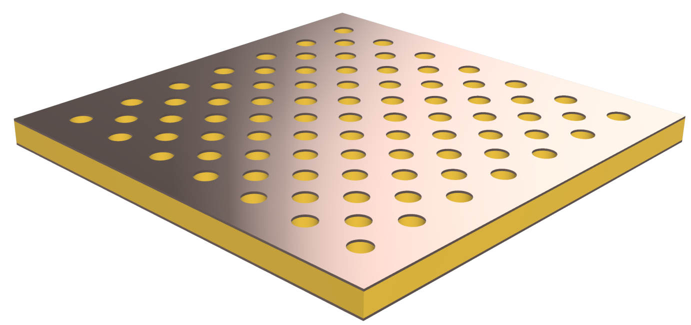

THGEM-like structure

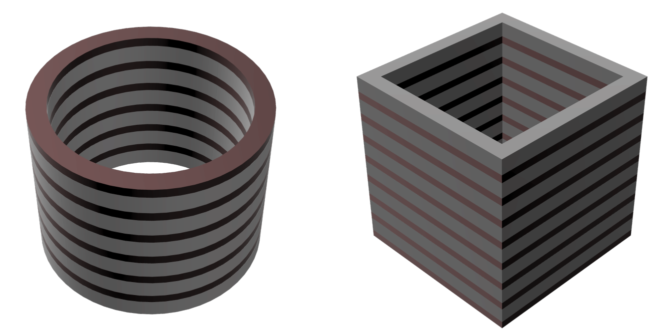

Arbitrary field shaper geometries

Technique:
Fused deposition modeling

Plastic filaments are heating in the moving head of a 3D printer and extruded through a thin nozzle. 3D objects are built up layer by layer in Z direction and the print head moves in XY across each layer.
Multiple extruding nozzles enable multi-colour or multi-material printing. This allows the usage of dissolvable support material or special materials such as electrically conductive carbon-loaded filaments.

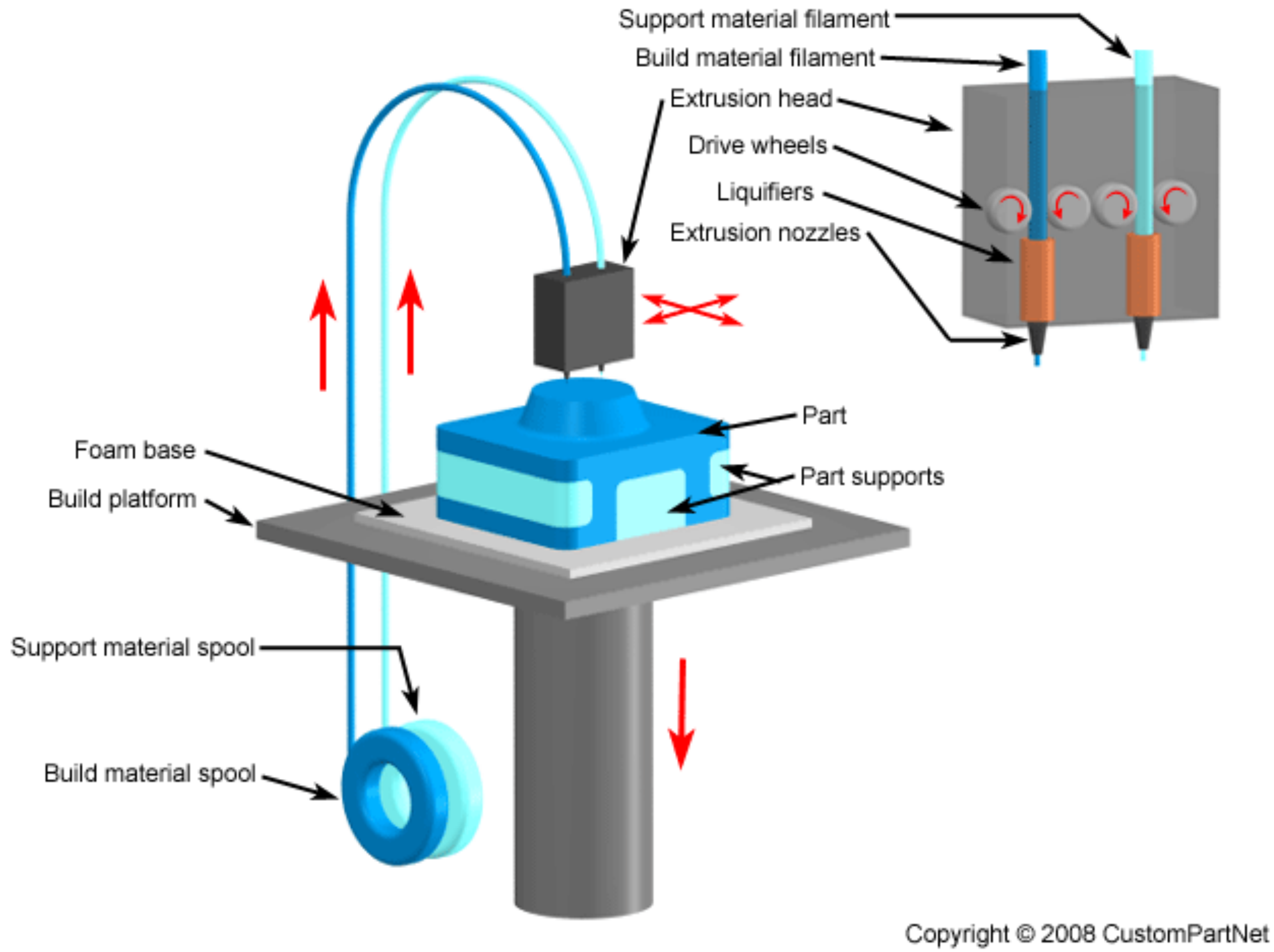

Image from: http://www.custompartnet.com/wu/fused-deposition-modeling

Outgassing

Vacuum

Outgassing measurements in vacuum available for 3D printed material

Data from:
NASA, "Outgassing Data for Selecting Spacecraft Materials"
https://outgassing.nasa.gov

Material	Total Mass Loss %
PEEK	0.14
FR4	0.27
PLA PLASTIC	0.56
ABS PLASTIC, 3D PRINTED	0.94
Kapton tape (siliconised)	1.5

Gas

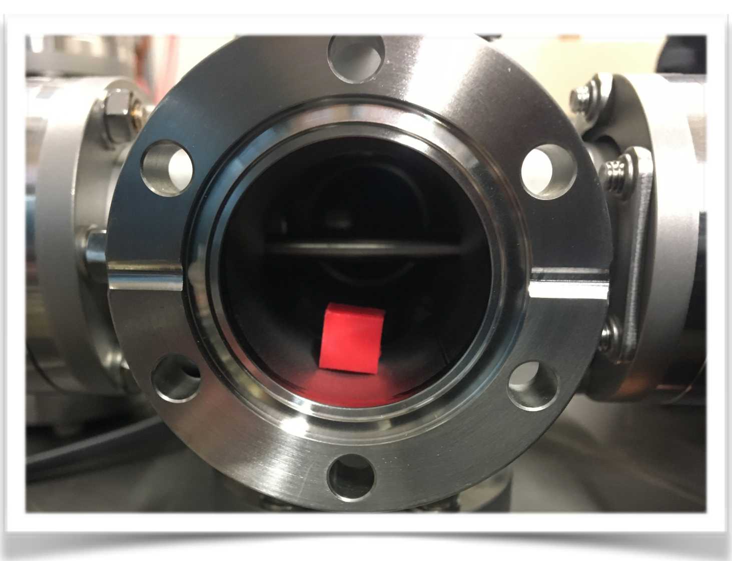

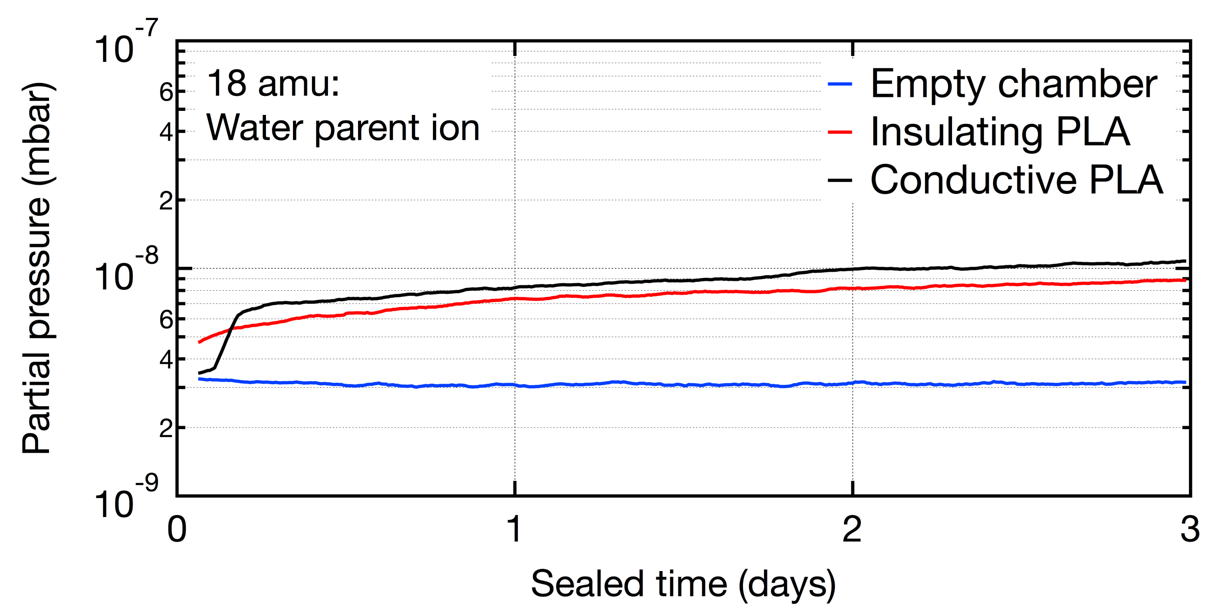

Test cubes ($1x1x1cm^3$) placed in UHV-grade vessel.
Some outgassing of water from both insulating as well as conductive PLA observable

Ionisation chamber

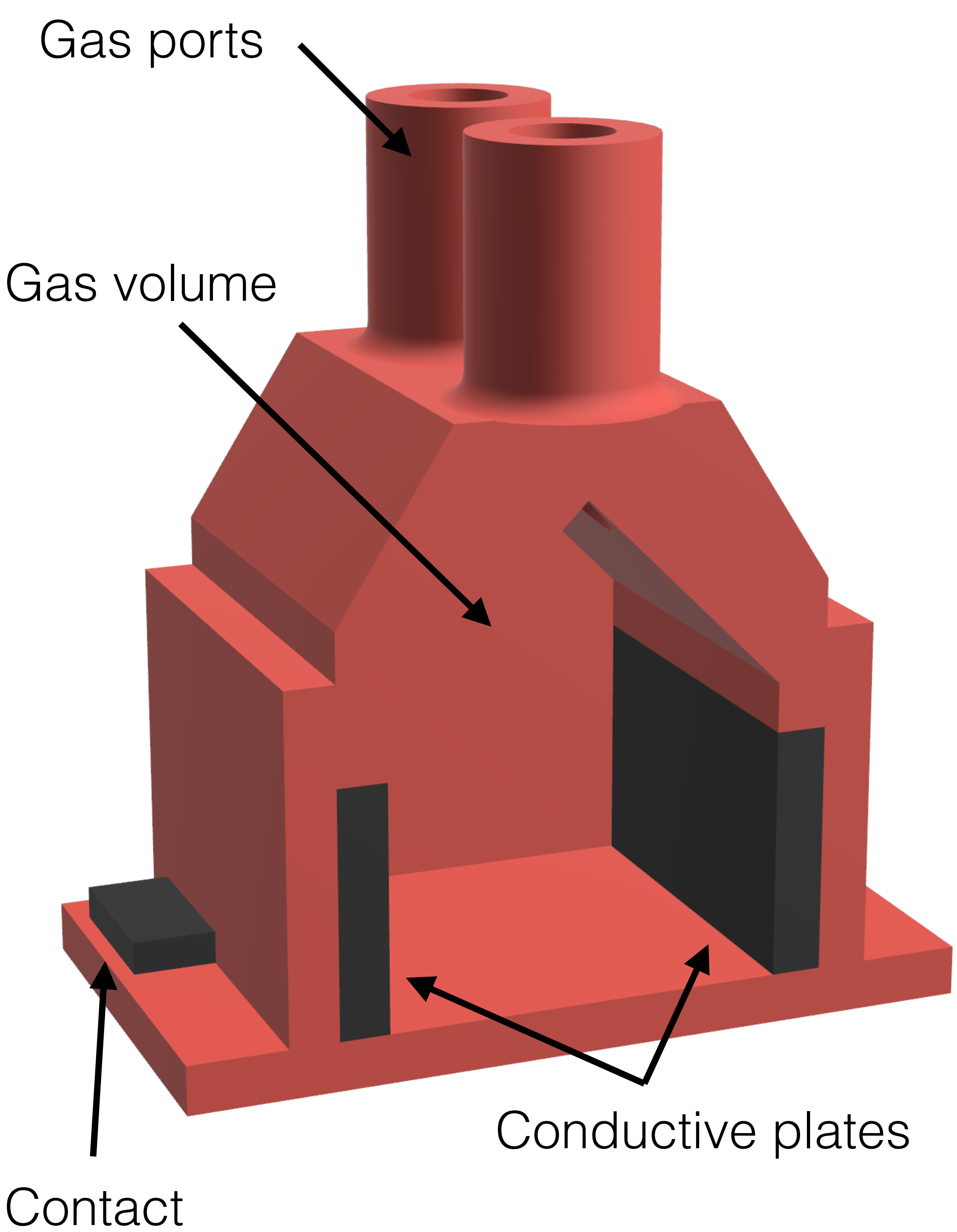

2 conductive plates (black) separated by 2cm

Housed in 3D printed gas volume made of insulating material (red)

Ionisation chamber

Printed overnight with 0.1mm layer height and slow speed for high surface quality

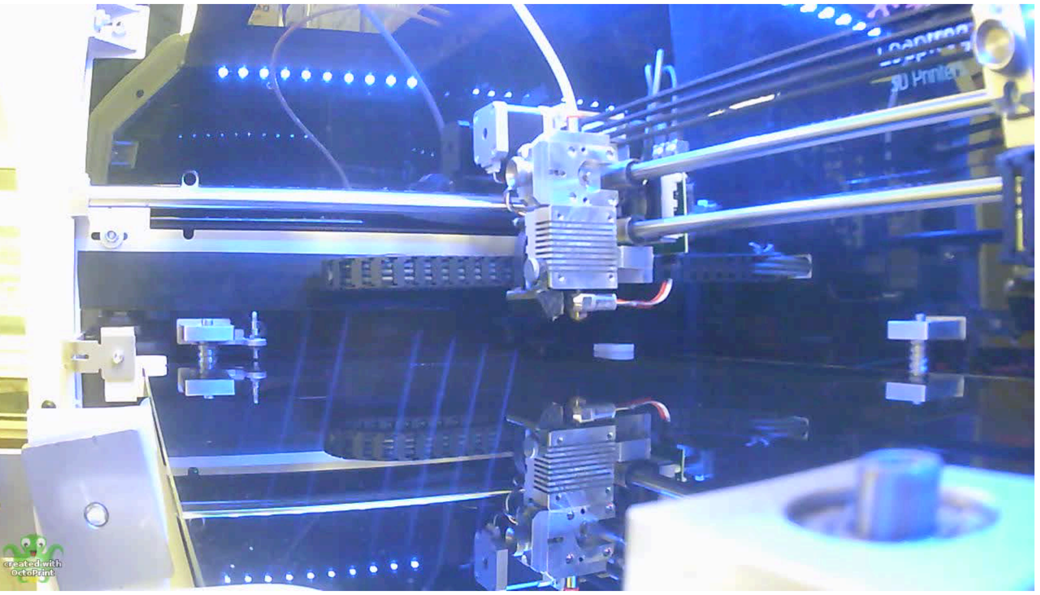

Timelapse of printing

IR-image during printing

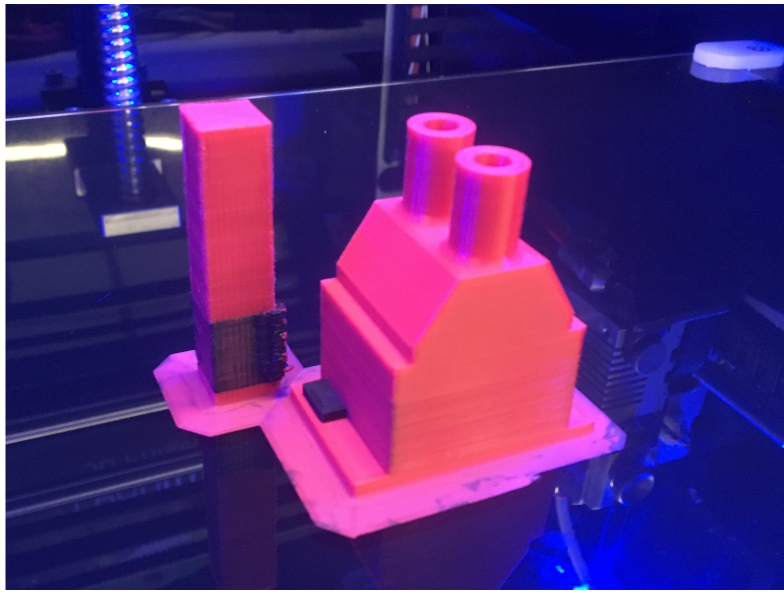

Finished print

Ionisation chamber

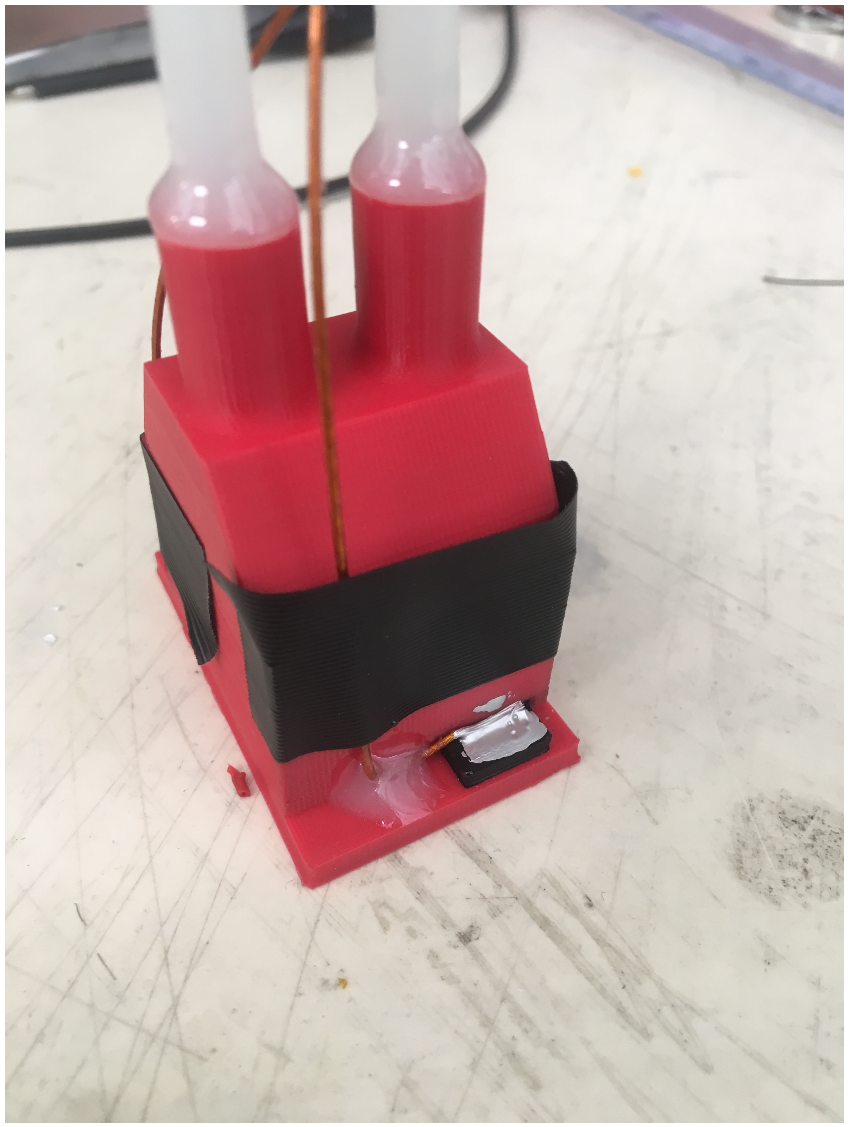

- 6mm tube inserted
- Fixed with glue
  Contact to conductive plates with Ag-loaded adhesive

Mounted in front of X-ray tube

Flushed with Ar at 5l/h (some leak of ≈1l/h)

One plate grounded through ammeter, other plate biased

Ionisation chamber

Recorded current depends linearly on the X-ray tube current i.e. X-ray intensity

Significant saturation / signal loss is observed for high X-ray intensity in the case of low drift fields

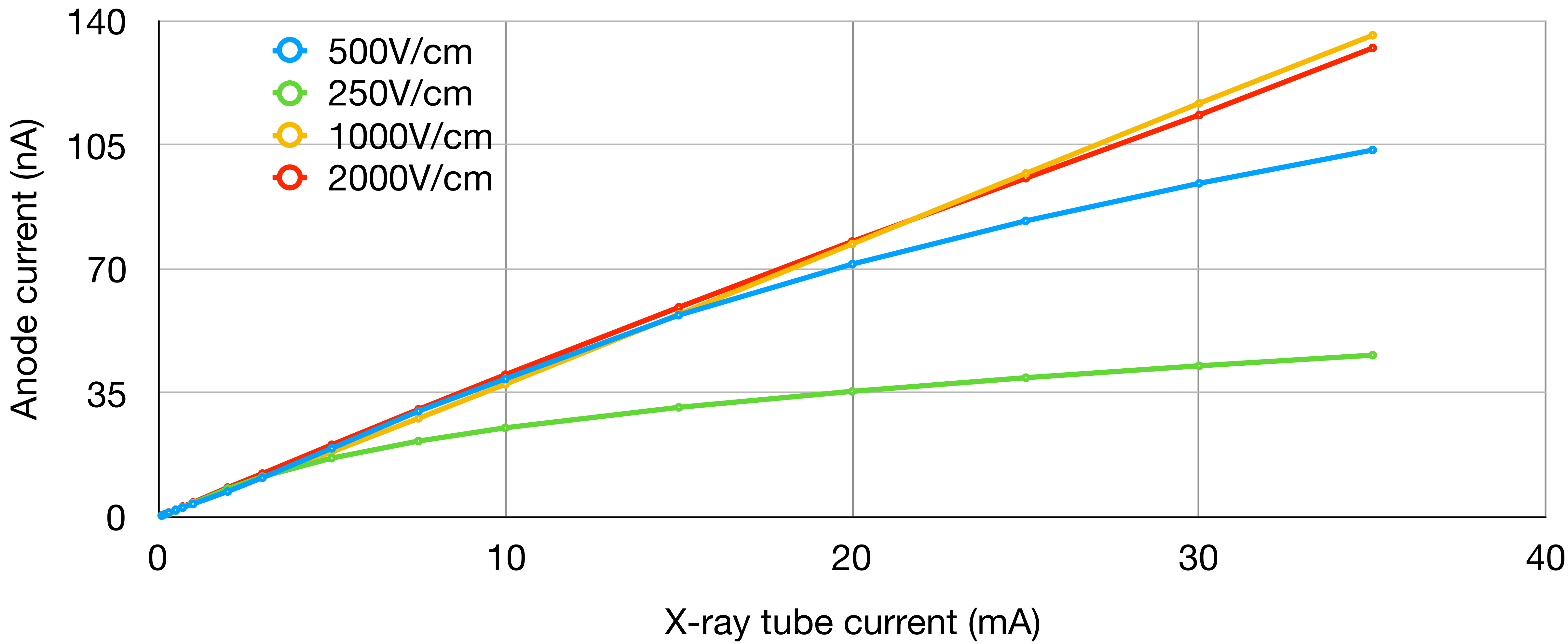

2D strip anode

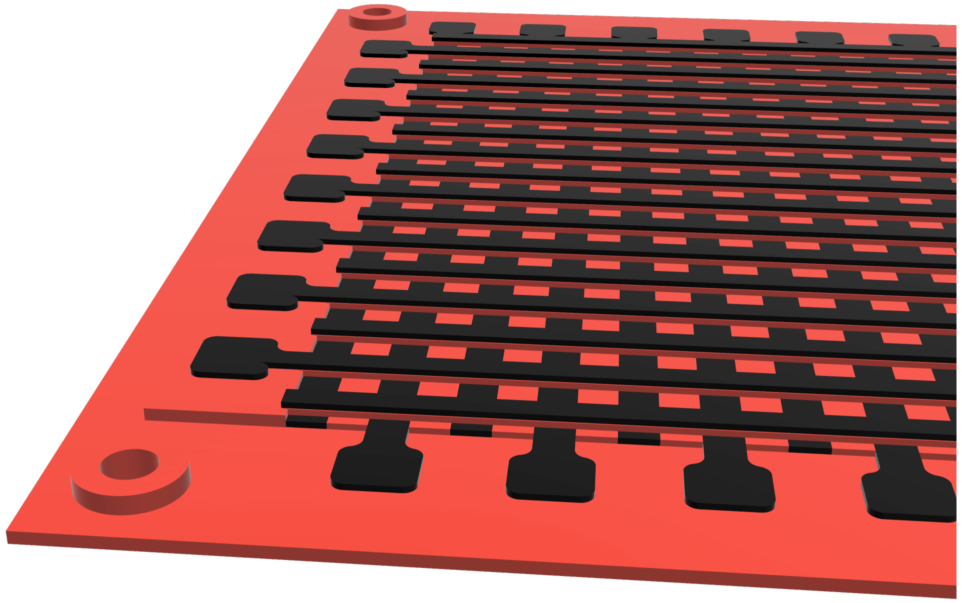
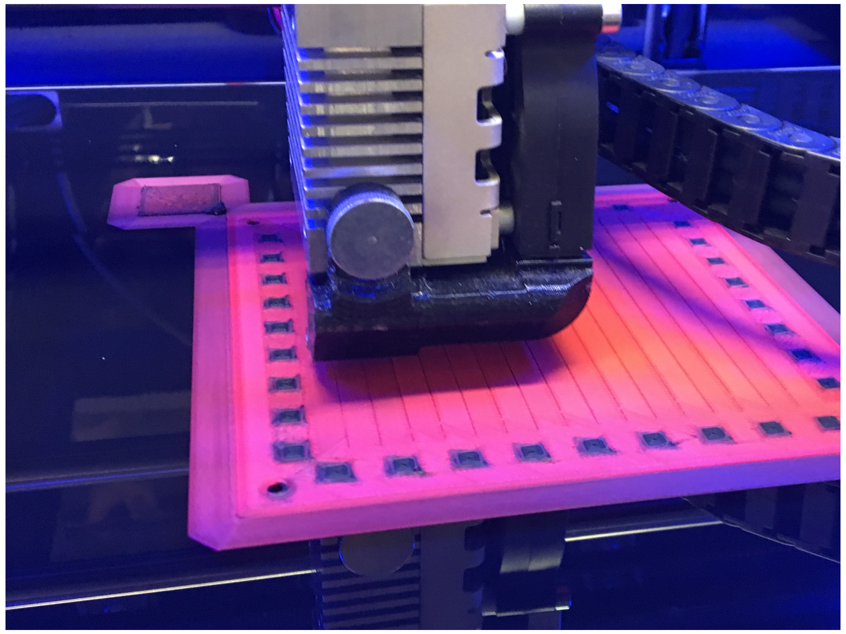
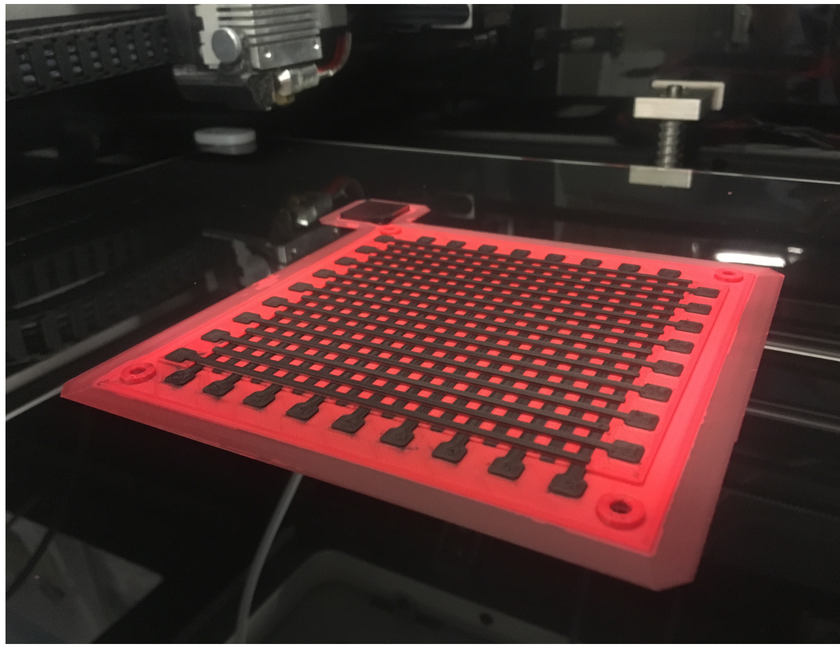

2 layers of strips separated by insulating material

Bottom strips: 3mm wide at 6mm pitch
Top strips: 2mm wide at 6mm pitch

Signal feedthrough to the back for contacting

18kΩ resistance along track
2-7kΩ resistance through contact feedthrough

2D strip anode

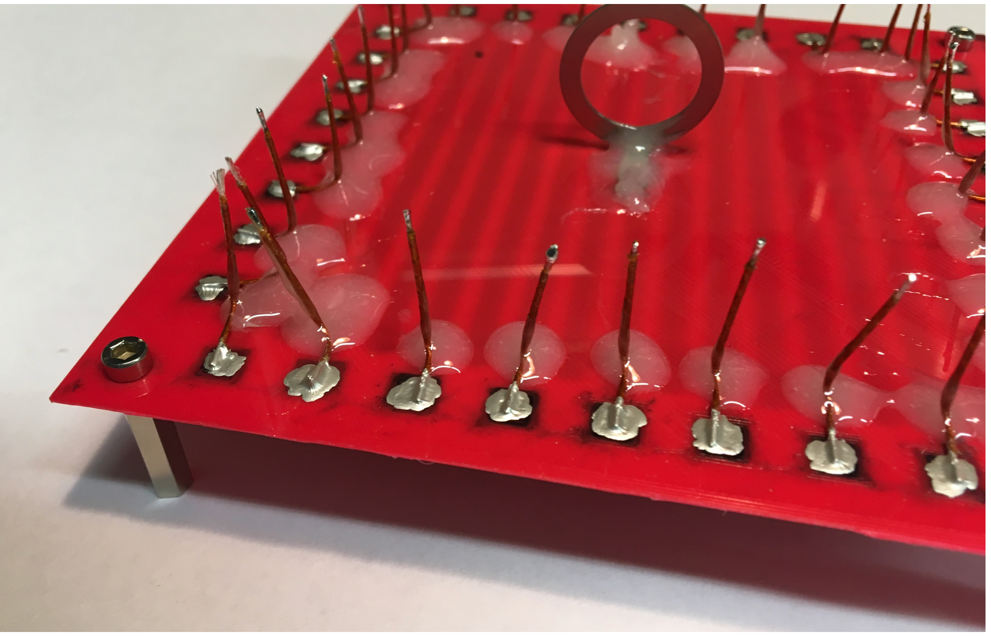 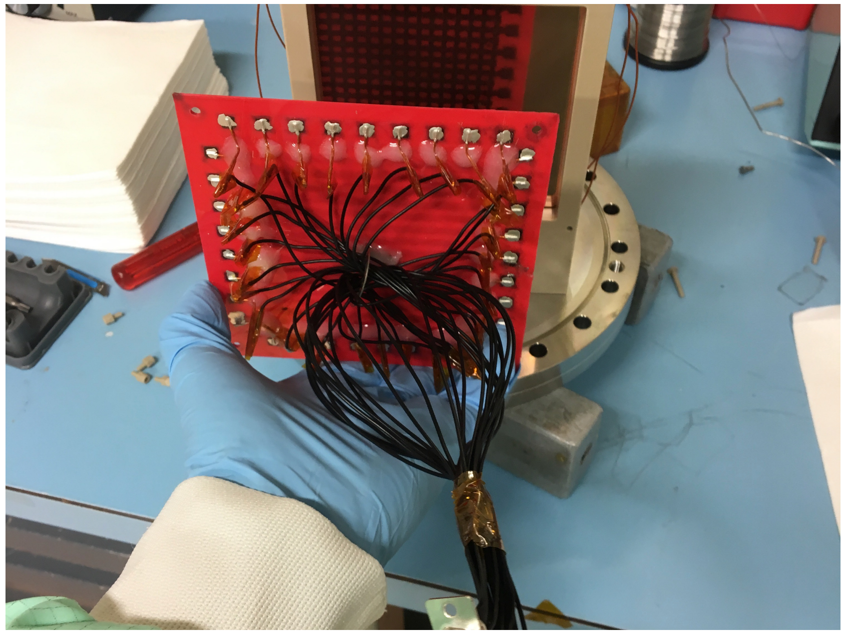 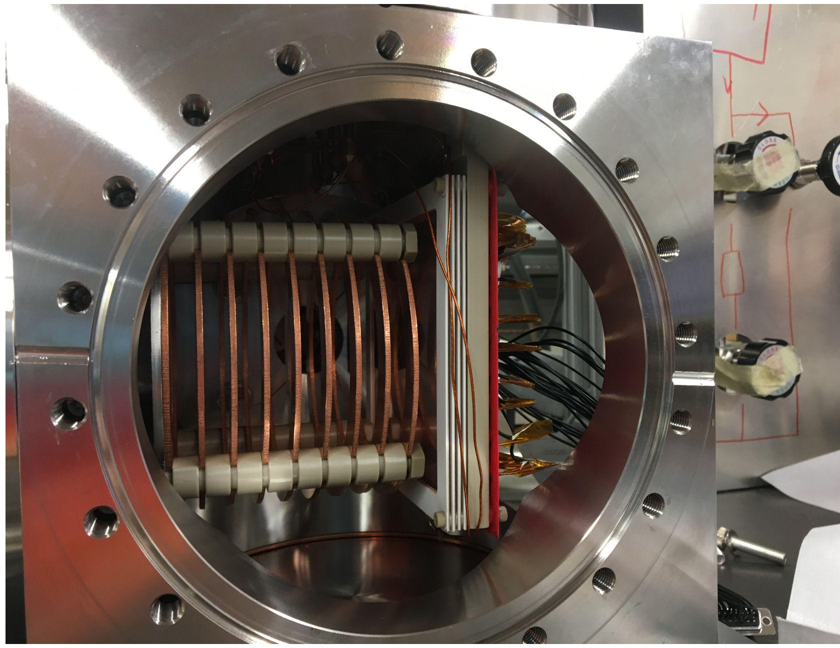

Contact pads on the back with Ag-based adhesive

Connected to D-Sub25 feedthrough

Mounted below quad-GEM stack with ≈1cm induction gap

2D strip anode

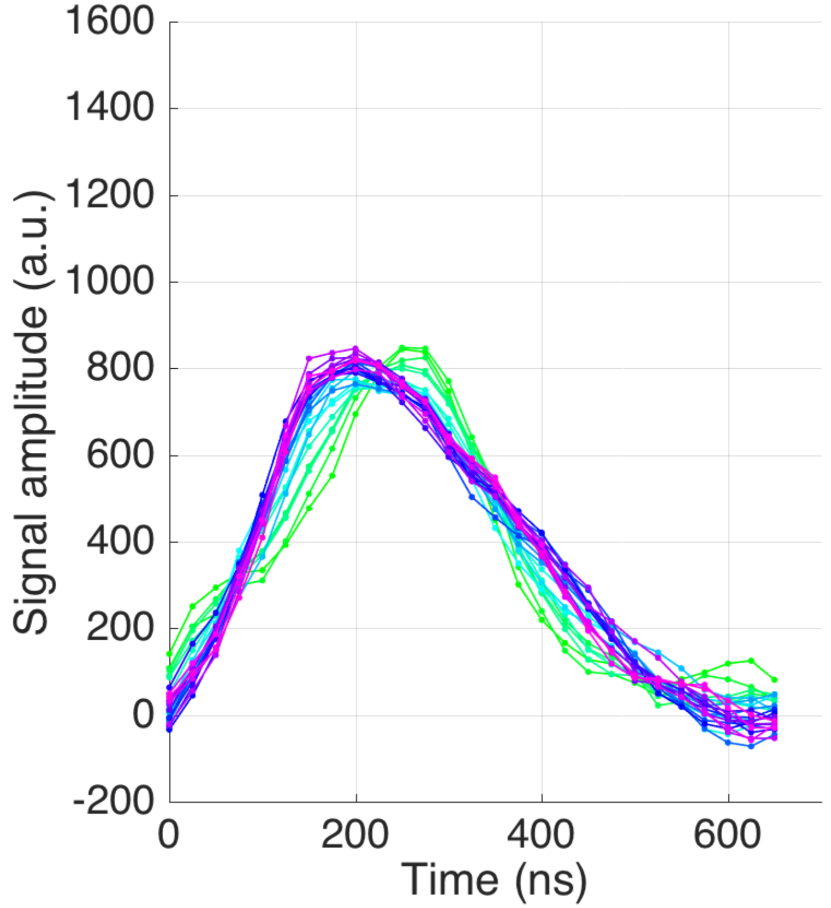

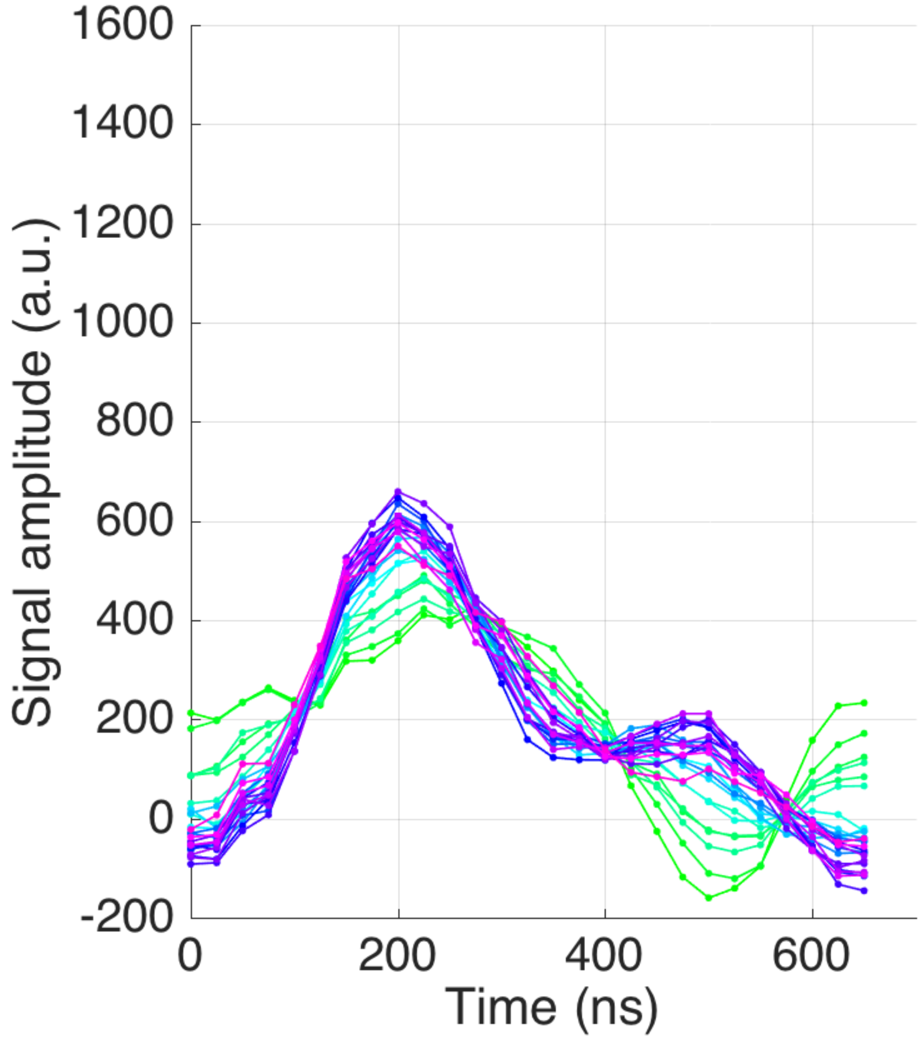

Electrical signals read out by APV25 connected to SRS

100 V/cm drift field
320 V across each GEM
200 V/cm induction field
4700x signal attenuation

Conclusions

Additive manufacturing of combined **conductive** and **insulating** structures may be useful for prototyping and manufacturing functional detector components

Fused filament fabrication (FFF) with **graphite-loaded filaments** can be used to fabricate **functional structures**

MPGD structures (e.g. THGEM) are **not accessible** by FFF due to limited resolution

Alternative technologies (e.g. conductive ink printing) could achieve necessary resolution

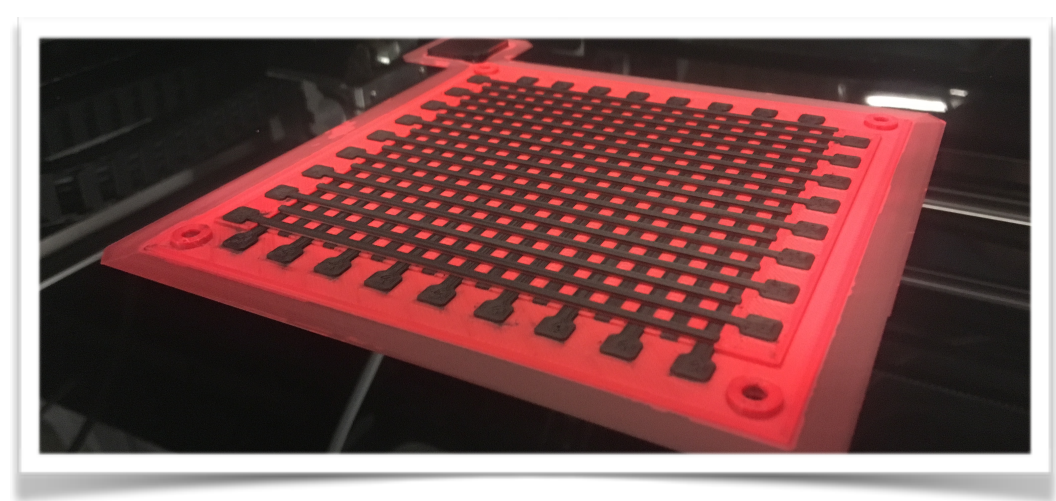

Thank you

Backup

High speed imaging

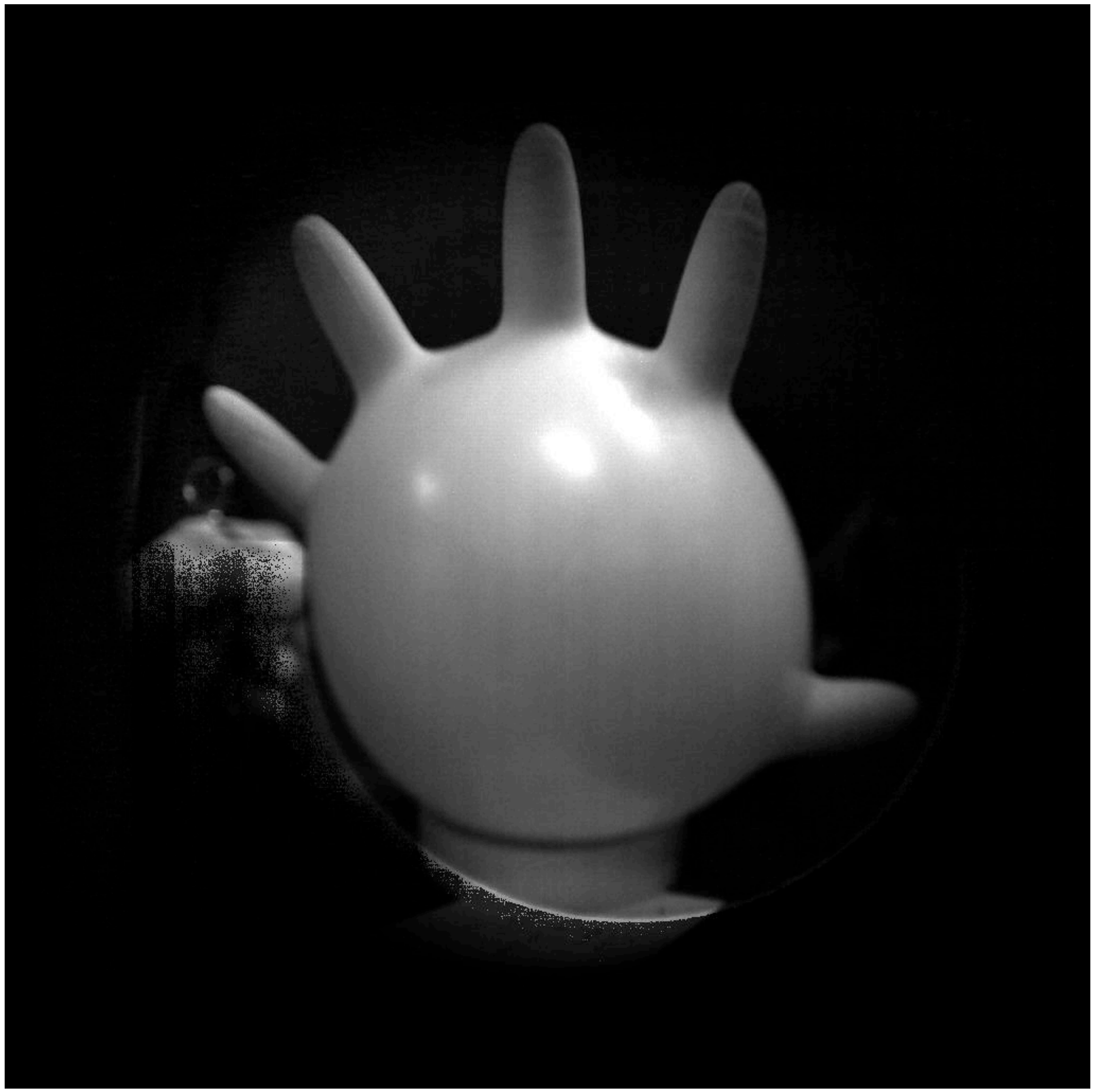

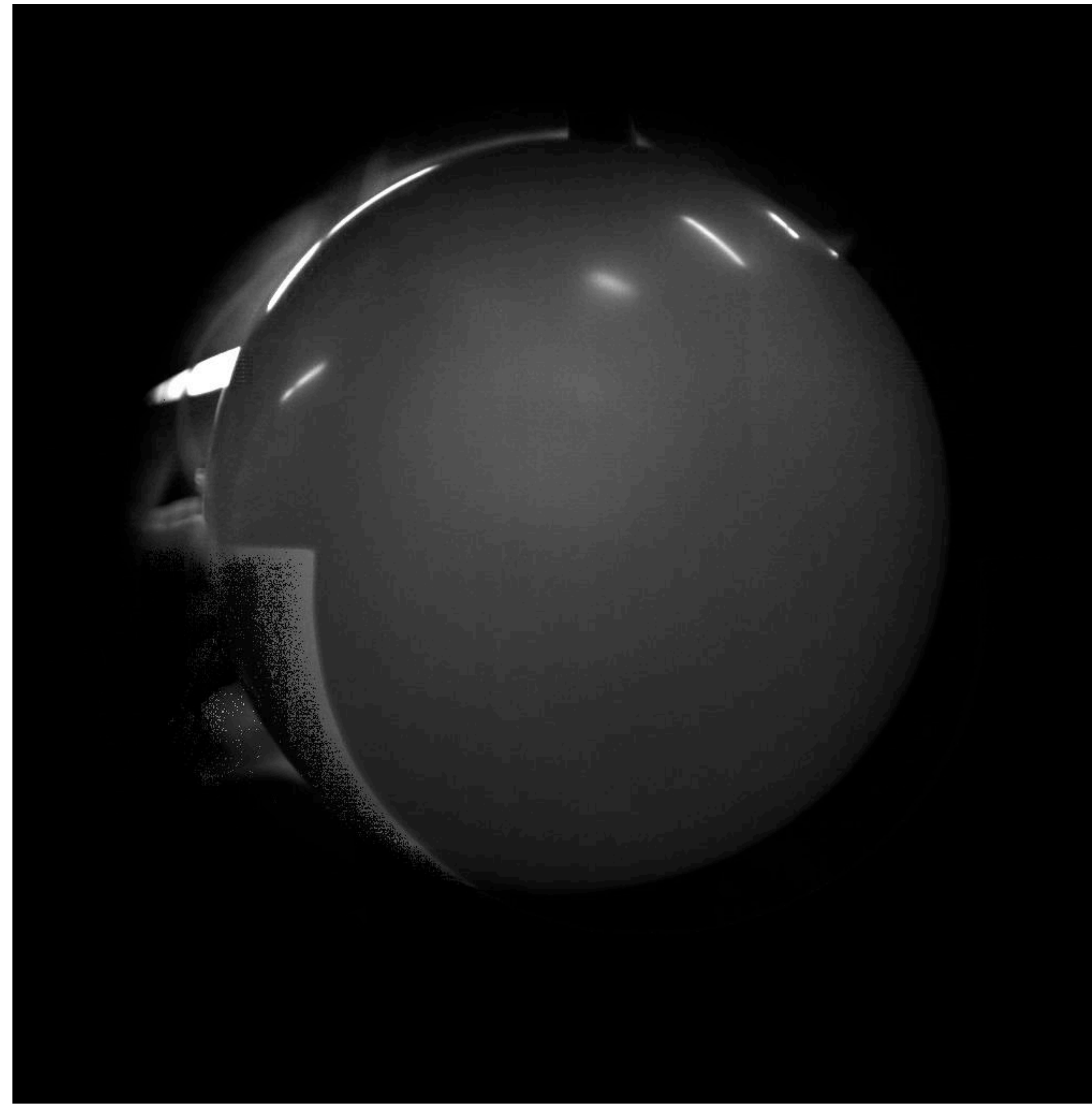

Popping baloon with 20kfps

Recording alpha tracks in TPC

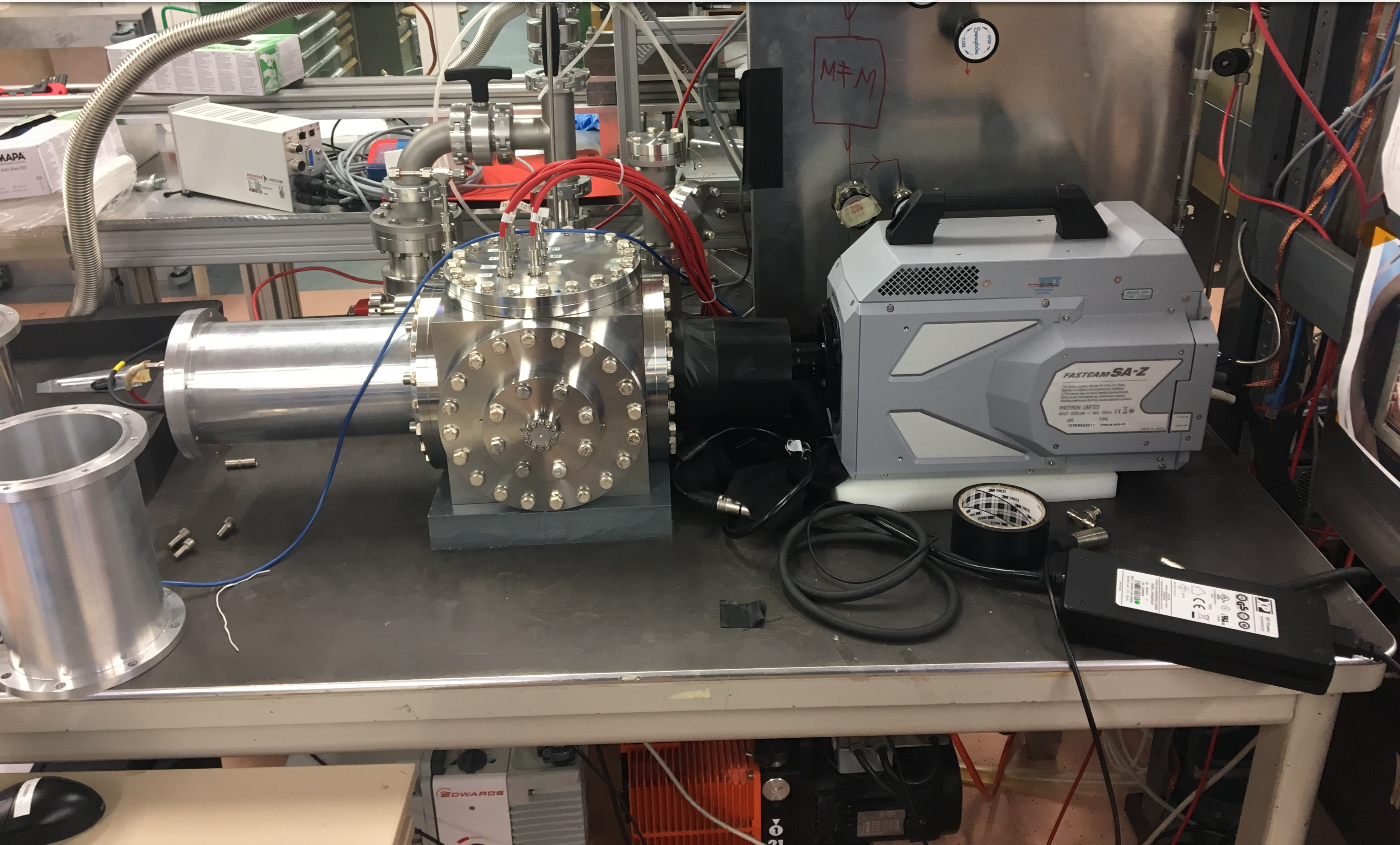

X-ray fluoroscopy

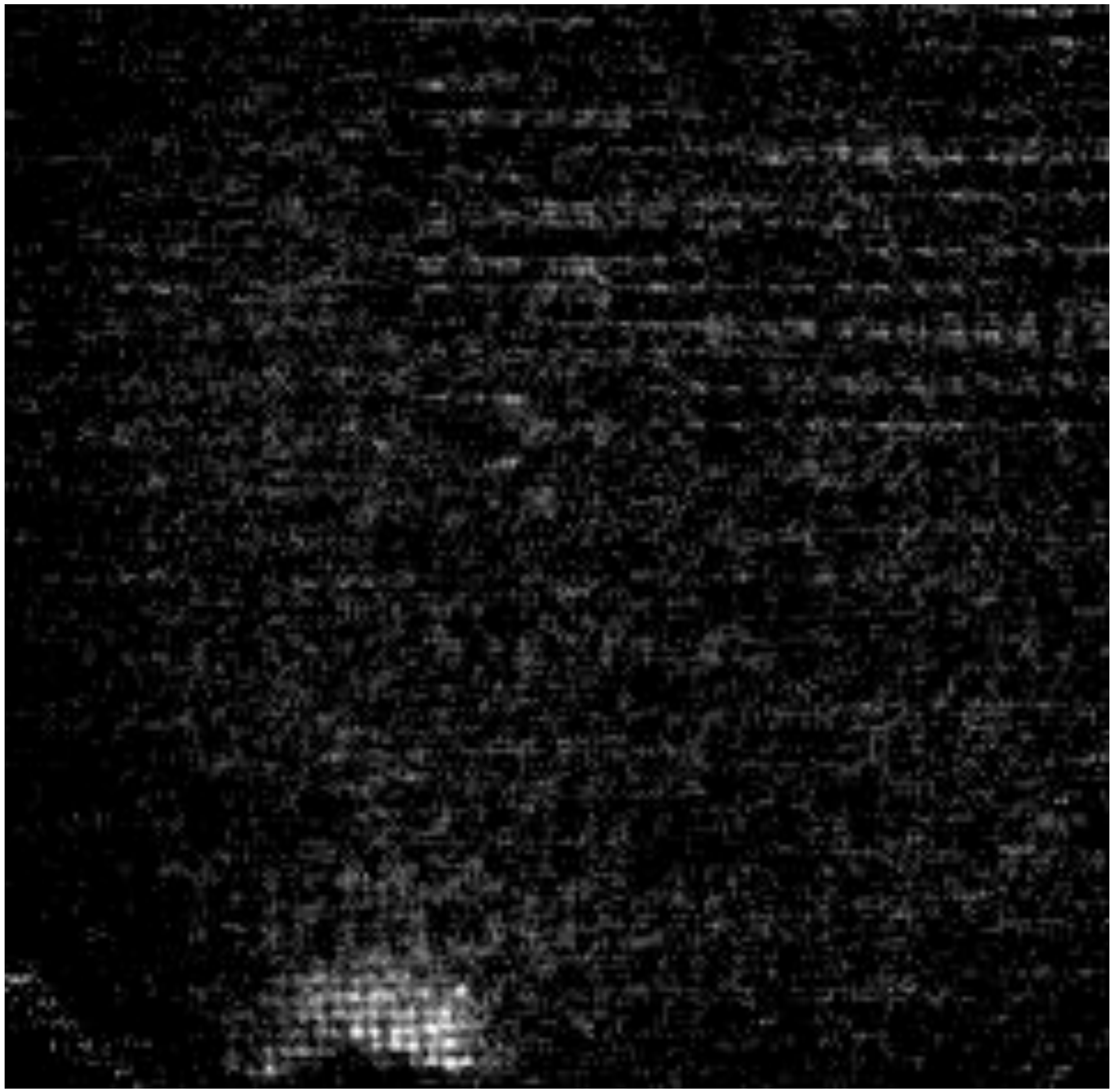

Bubbles in water, recorded at 5 kfps, displayed at 1/50 speed

X-ray fluoroscopy

Remote controlled Blade drone in paper cylinder in front of detector irradiated with X-ray tube

Phantom high speed camera

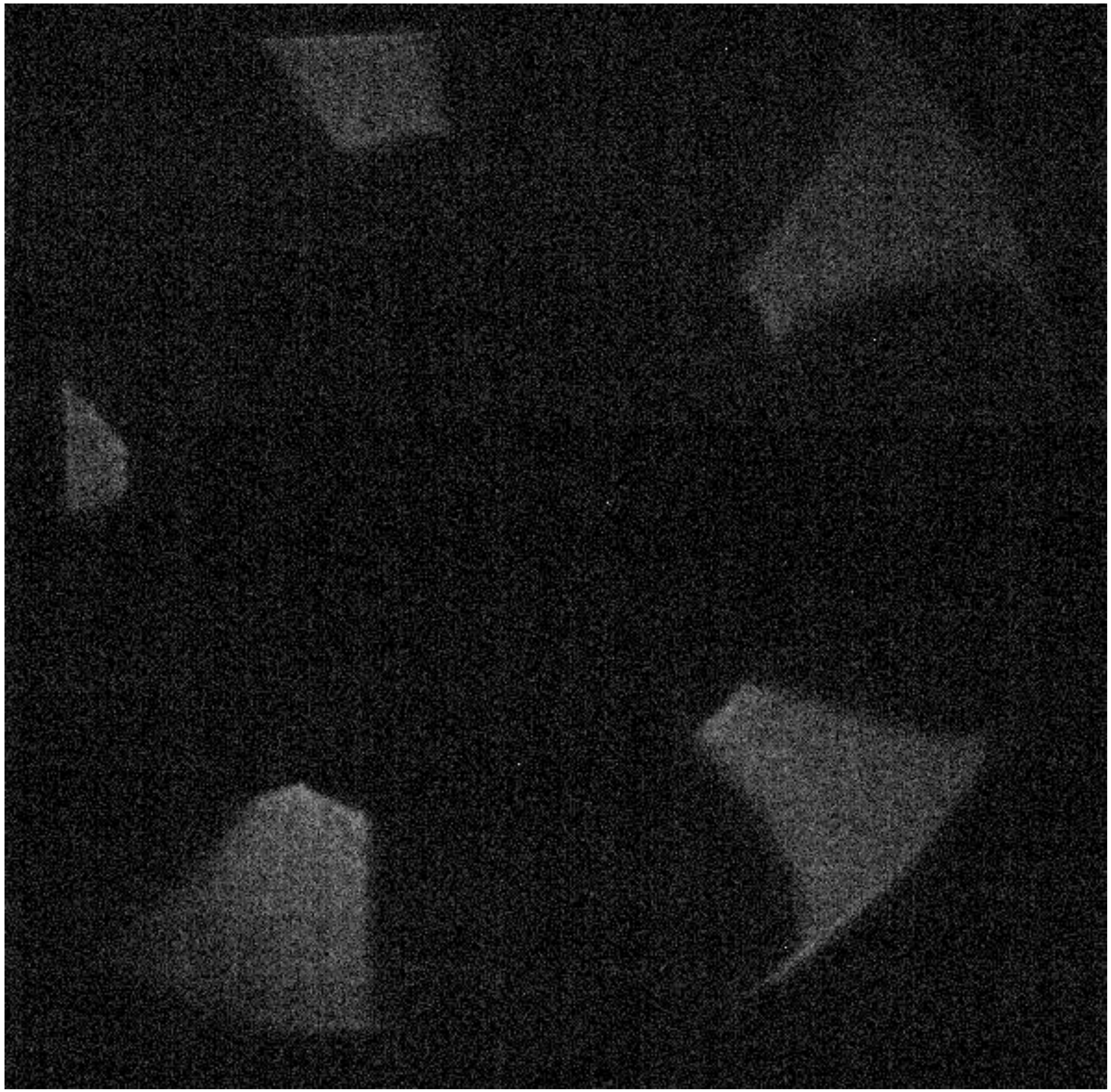

Hadron therapy

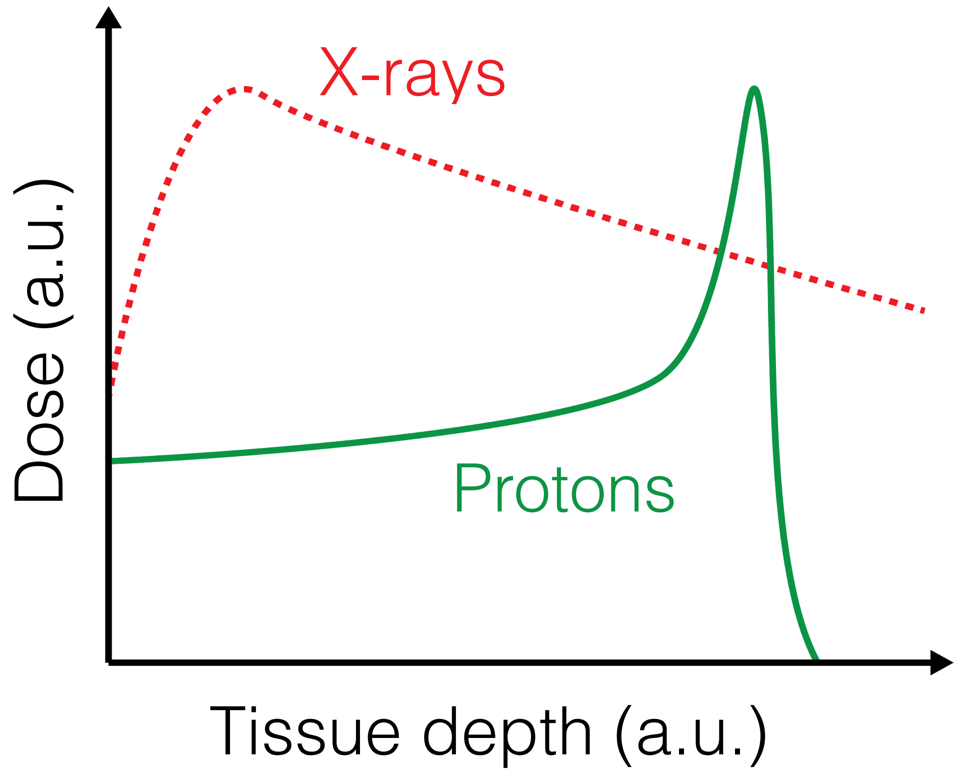

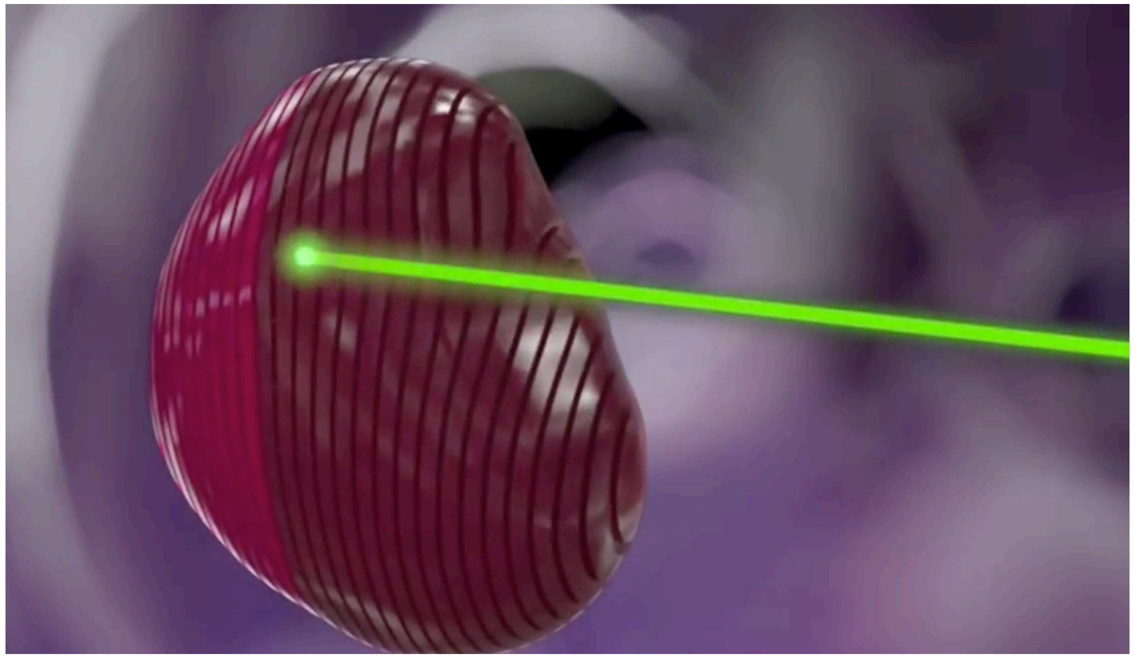

Adapted from iba Proton Therapy
https://www.youtube.com/watch?v=MS590Xtq9M4&t=5s

Hadron therapy allows selective targeting of cancerous tissue

Scanning pencil beam delivers dose according to patient-specific treatment plan

Schematics not drawn to scale

State-of-the-art

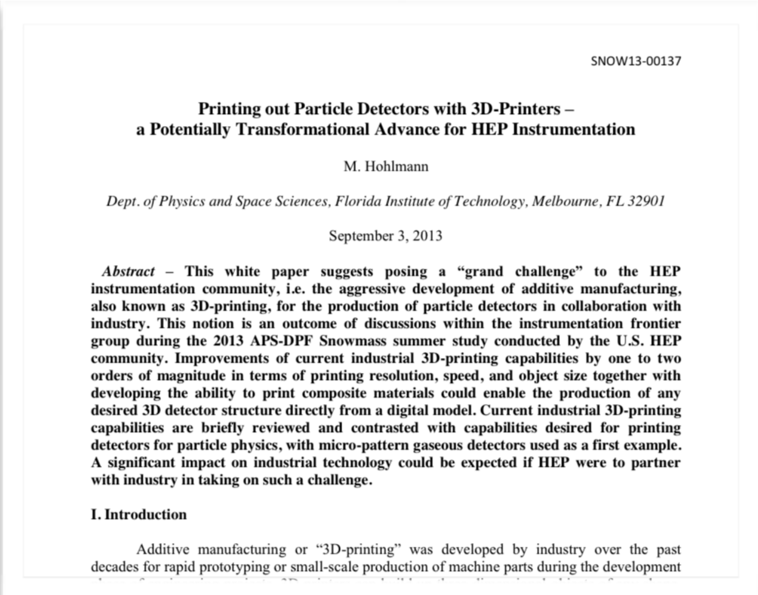

SNOW13-00137

Printing out Particle Detectors with 3D-Printers –
a Potentially Transformational Advance for HEP Instrumentation

M. Hohlmann

Dept. of Physics and Space Sciences, Florida Institute of Technology, Melbourne, FL 32901

September 3, 2013

Abstract **– This white paper suggests posing a "grand challenge" to the HEP instrumentation community, i.e. the aggressive development of additive manufacturing, also known as 3D-printing, for the production of particle detectors in collaboration with industry. This notion is an outcome of discussions within the instrumentation frontier group during the 2013 APS-DPF Snowmass summer study conducted by the U.S. HEP community. Improvements of current industrial 3D-printing capabilities by one to two orders of magnitude in terms of printing resolution, speed, and object size together with developing the ability to print composite materials could enable the production of any desired 3D detector structure directly from a digital model. Current industrial 3D-printing capabilities are briefly reviewed and contrasted with capabilities desired for printing detectors for particle physics, with micro-pattern gaseous detectors used as a first example. A significant impact on industrial technology could be expected if HEP were to partner with industry in taking on such a challenge.**

I. Introduction

Additive manufacturing or "3D-printing" was developed by industry over the past decades for rapid prototyping or small-scale production of machine parts during the development

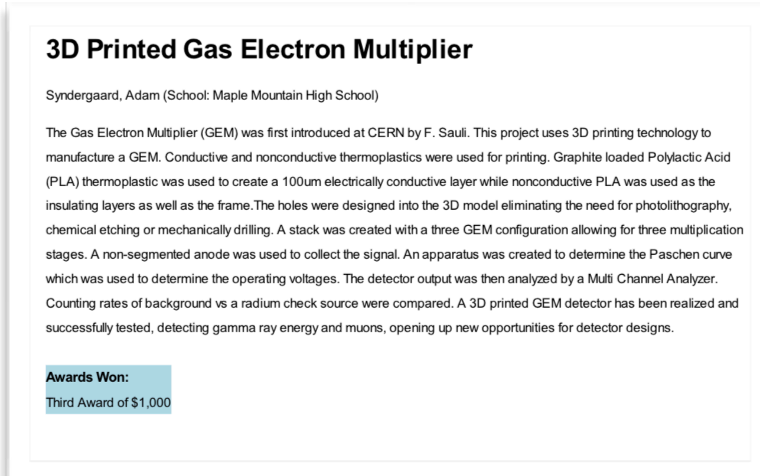

3D Printed Gas Electron Multiplier

Syndergaard, Adam (School: Maple Mountain High School)

The Gas Electron Multiplier (GEM) was first introduced at CERN by F. Sauli. This project uses 3D printing technology to manufacture a GEM. Conductive and nonconductive thermoplastics were used for printing. Graphite loaded Polylactic Acid (PLA) thermoplastic was used to create a 100um electrically conductive layer while nonconductive PLA was used as the insulating layers as well as the frame.The holes were designed into the 3D model eliminating the need for photolithography, chemical etching or mechanically drilling. A stack was created with a three GEM configuration allowing for three multiplication stages. A non-segmented anode was used to collect the signal. An apparatus was created to determine the Paschen curve which was used to determine the operating voltages. The detector output was then analyzed by a Multi Channel Analyzer. Counting rates of background vs a radium check source were compared. A 3D printed GEM detector has been realized and successfully tested, detecting gamma ray energy and muons, opening up new opportunities for detector designs.

Awards Won:
Third Award of $1,000

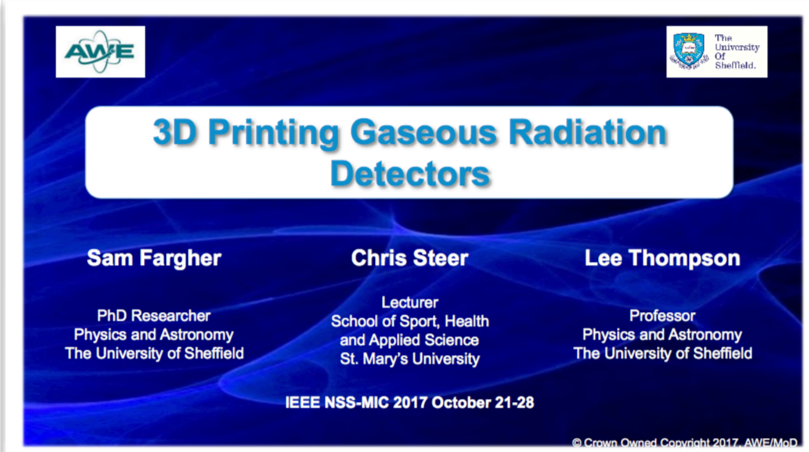

M. Hohlmann (Florida Tech) arXiv paper (2013)

Conceptual ideas but no realisation

https://arxiv.org/pdf/1309.0842.pdf

3D printed GEM claimed in US high school student competition (2017)

no further info found

L. Thompson et al. (Sheffield University)

"3D Printing Gaseous Radiation Detectors" IEEE NSS 2017

3D printed box housing single wires

Smoothing of PLA

Tried smoothing PLA printed parts in ethyl acetate

Parts dissolved and reaction to conductive and insulating PLA was different

Not suitable to smooth printed parts

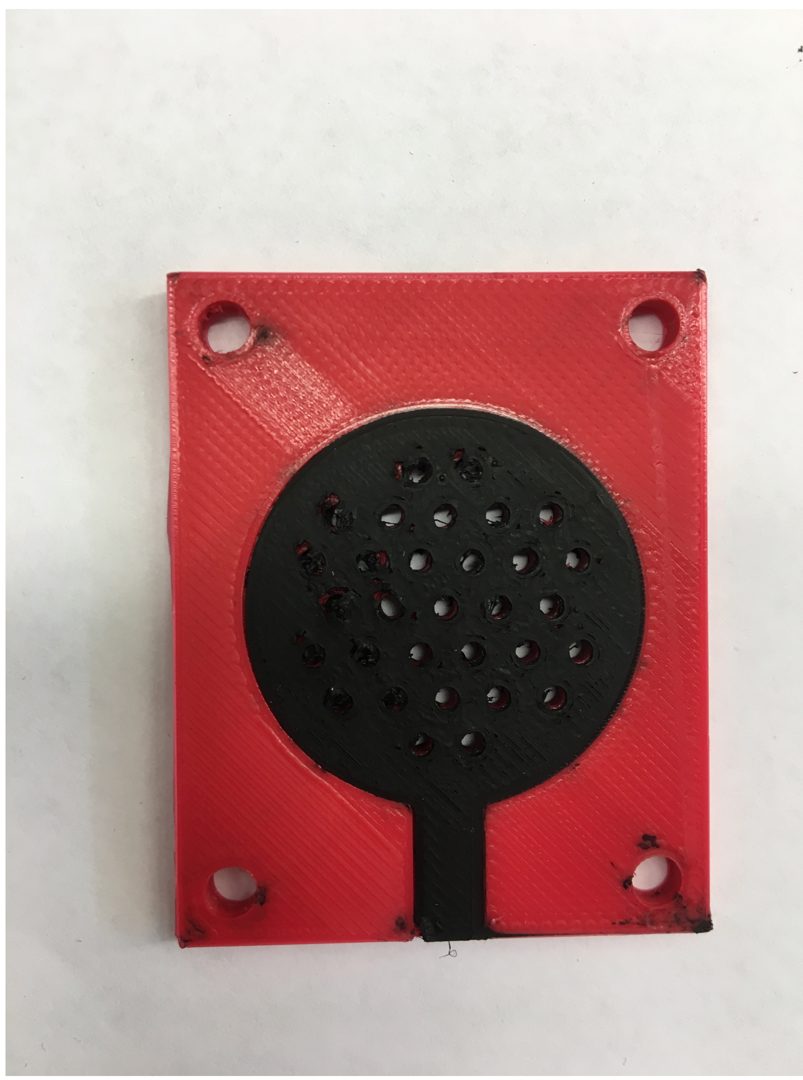

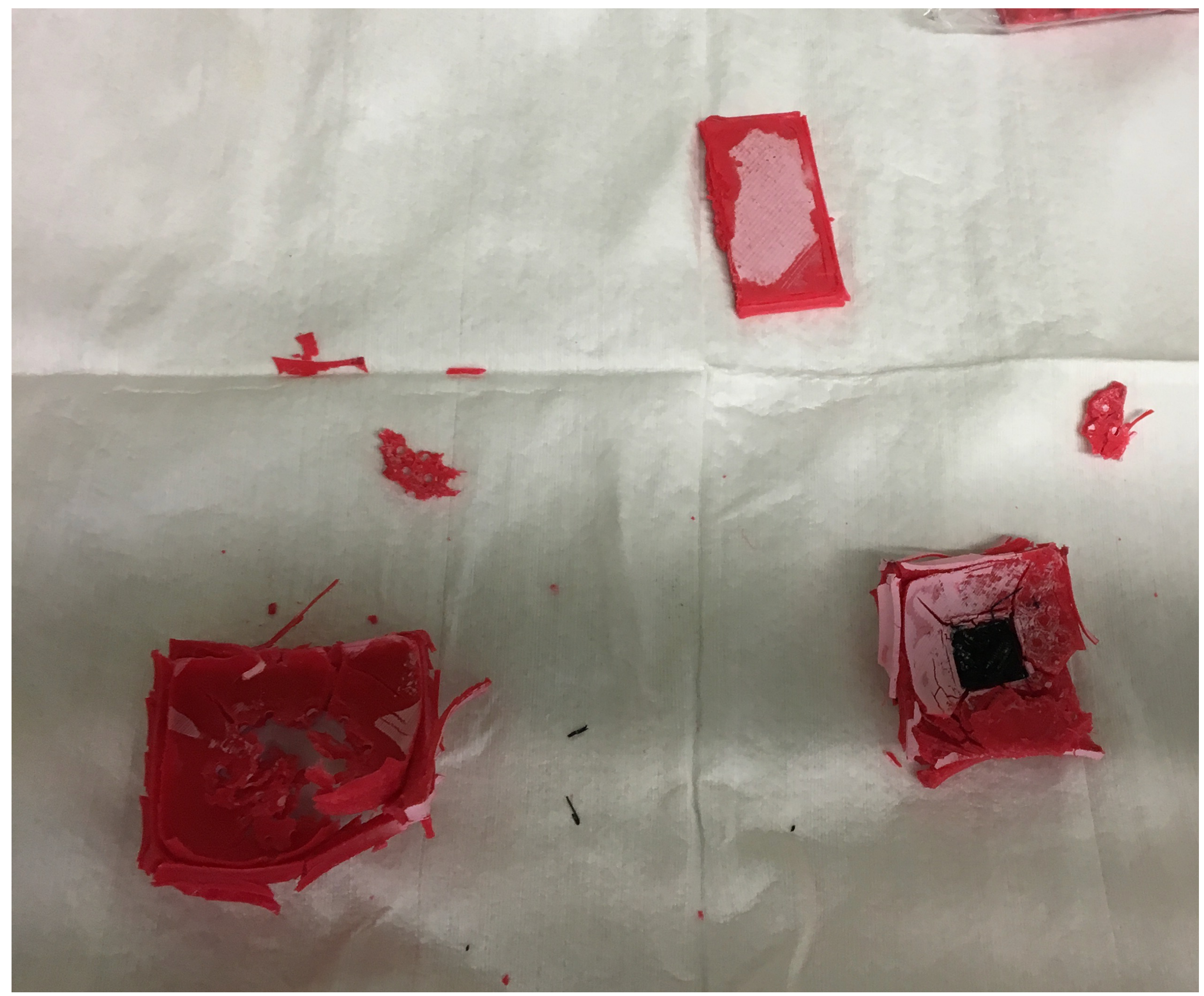

1D strip anode

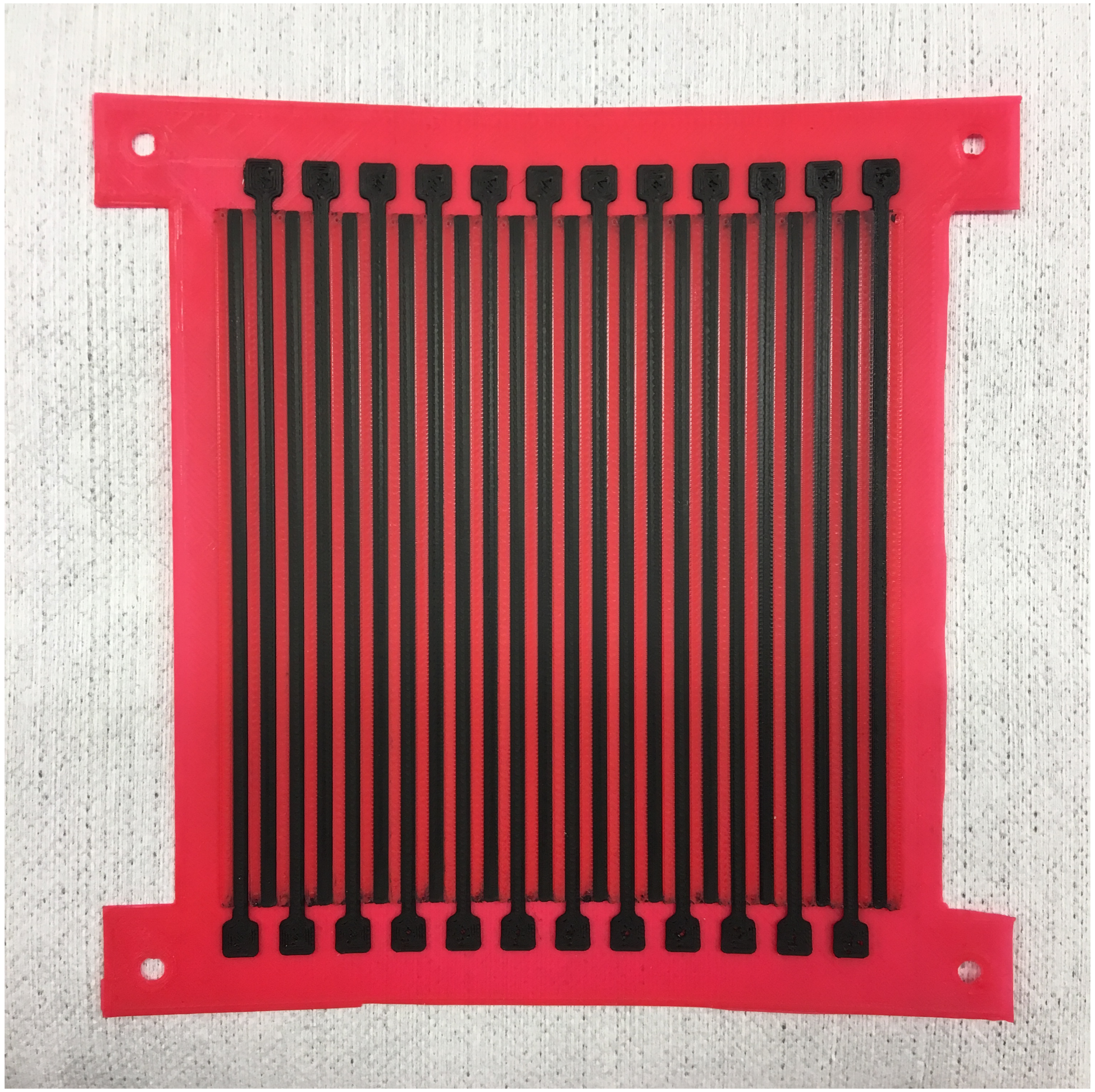

1D strip anode for 10x10 cm^2 active area

2mm wide strips with a pitch of 4mm

Outgassing

Compatibility of PLA outgassing with gaseous detectors in open gas flow mode needs to be evaluated but seems feasible from available outgassing numbers compared to other commonly used materials

Material	Total Mass Loss %	Collected Volatile Condensable Materials
PEEK	0.14	0.00
FR4	0.27	0.00
PLA PLASTIC	0.56	0.01
ABS PLASTIC, 3D PRINTED	0.94	0.04
Kapton tape (siliconised)	1.5	0.52
Araldite 2020	2.17	0.10

Outgassing measurements in vacuum. Data from:
NASA, "Outgassing Data for Selecting Spacecraft Materials", https://outgassing.nasa.gov, Accessed February 26, 2018